ABSTRACT

Title of thesis: DEVELOPMENT AND CLINICAL TESTING OF
                    A TIME-EFFICIENT METHOD FOR
                    TRIANGULATING THE VENTRICULAR
                    TACHYCARDIA SITE OF ORIGIN TO SUPPORT
                    CARDIAC ABLATION PROCEDURES

                    Joseph Samuel Davis, Master of Science, 2012

Thesis directed by: Professor Keith E. Herold, Research Advisor

This thesis presents a ventricular tachycardia source of origin (VTSO) localization algorithm that assists electrophysiologists during cardiac ablation (CA) procedures. The algorithm uses a linear relationship of electrocardiogram (ECG) similarity and distance between pace mapping (PM) points to identify a small (<6% of total surface area) target region on the ventricle containing the VTSO. An average ventricular linear regression (AVLR) guides PM point selection, a cross-correlation sum algorithm automatically extracts the QRS segment of VT ECGs for analysis, and a surface reconstruction algorithm forms ventricular surface models to visualize results. Retrospective studies using clinical data from 21 patients acquired a target region using between 3 and 5 PM points total, compared with normal pace mapping procedures that require more than 20 PM points. The algorithm should significantly decrease CA procedure time, reducing the total physical stress on the patient's heart while also reducing operating costs for both patients and hospitals.

DEVELOPMENT AND CLINICAL TESTING OF A TIME-EFFICIENT METHOD FOR TRIANGULATING THE VENTRICULAR TACHYCARDIA SITE OF ORIGIN TO SUPPORT CARDIAC ABLATION PROCEDURES

by

Joseph Samuel Davis

Thesis submitted to the Faculty of the Graduate School of the
University of Maryland, College Park in partial fulfillment
of the requirements for the degree of
Master of Science
2012

Advisory Committee:

      Associate Professor Keith E. Herold, Chair
      Associate Professor Adam Hsieh
      Assistant Professor Santiago Solares

Table of Contents

Table of Figures

iv

List of Tables

Chapter 1 – Introduction

Ventricular tachycardia (VT) is a fast heart rhythm originating in the ventricles of the heart that can lead to ventricular fibrillation, asystole (i.e. flatlining), sudden cardiac arrest, and congestive heart failure (CHF). The American Heart Association reported that in the United States alone, CHF is prevalent in 5.7 million people with 56,565 mortalities in 2007 [1]. Approximately 90% of patients who present VT contain obvious signs of cardiomyopathy, i.e. structural heart disease - a subset of cardiovascular disease (CVD) [2]. The total annual direct and indirect costs of this diagnostic group were estimated at $286 billion, higher than any other including cancer [1].

Treatment options for VT range from prescription medications, to implantable defibrillators or pacemakers, to cardiac ablation (CA) procedures. For treating VT, these CA procedures can take up to 6 or more hours. The lengthy procedures put stress on the hearts of the patients, resulting in additional recovery time and possible complications. The long procedure time also limits the total number of CA procedures that can be performed per day. Extended procedure times increase hospital costs which are often pushed onto the patient, e.g. $30,000 to over $50,000 depending on the length of the procedure and equipment required [3]. Additionally, every minute if operating time exposes the surgeons, nurses, technicians, anesthesiologists, and patient to nearby x-ray radiation, increasing their risk of developing cancer. Many of these problems could be mitigated by reducing procedure time.

The length of a VT ablation procedure depends largely on how quickly the surgeon can pinpoint the VT site of origin (VTSO) as the target for ablation. An

1

algorithm that could quickly locate the VTSO would significantly reduce the total physical stress on the patient and staff as well as reduce medical costs. While several algorithms have been previously developed, a real time method leading to a focused and unique target region containing the VTSO has remained illusive.

A current widespread method used by doctors in locating the VTSO is known as electrocardiographic pace mapping (PM). The method involves electrically stimulating, or pacing, the ventricle at a specific point while monitoring the resultant electrocardiogram (ECG). Based on the morphological and timing differences between the PM ECG and the known ECG of a VT event, the physician mentally calculates the location of the next pacing point and then paces at the new location. When the ECG of a PM point is a close match to that of the clinical VT, the location is interpreted as the VTSO. This method requires extensive experience to perform efficiently, involves trial and error, and requires repeated pacing of the heart. Pace mapping often requires more than 20 PM points and in many cases the VTSO remains elusive. In these situations, the surgeon may switch to voltage mapping or activation mapping, separate procedures that add additional hours to the total operating time. The purpose of the current study is to create an algorithm and method to automate the location of the VTSO from limited pacing data which should significantly reduce the total operating time of the ablation procedure.

Algorithms previously developed to assist physicians in quickly locating the VTSO have been limited to specific situations, are non-real time, and rely on general heart models or computed tomography (CT) scans of the heart. They also limit the AoP for the VTSO to a generalized location of the ventricle instead of a focused and unique

area for each particular patient. The algorithms developed by Segal et al. and Ito et al. successfully determined general VTSO locations based on ECG characteristics [4, 5]. However, these two methods use pre-defined regions within the heart when identifying a VTSO location such as the basal mid-posterior or RV-septum, respectively (see Chapter 2 for heart anatomy). An algorithm developed by Sanroman-Junquera et al. uses stored ECG's from a patient's implanted defibrillator. However, this approach is limited to a small niche of patients who already have an implanted defibrillator. Furthermore, it localizes the AoP of the VTSO to one of eight predefined octants of the ventricle, doing so with only 36.3% accuracy [6]. A different method designed by Zheng et al. does not require catheters for mapping the VTSO location, but does involve CT scans of the heart acquired in advance [7]. The CT scans and extra electrodes for this method make it more difficult to introduce into standard CA procedures. An algorithm that rapidly localizes the VTSO to a unique and focused region of the heart is still needed.

One of the main challenges with the development of such an algorithm is the complexity of the heart's electrical conduction pathways. Adding to this complexity is the common existence of scar tissue regions within the hearts of cardiac ablation patients. These unavoidable factors can cause high variation in recorded data which leads to the low accuracy of some algorithms like that of Sanroman-Junquera et al. [6]. Therefore, a useful algorithm must be robust, allowing for this expected variance and correcting or negating potential errors with simple and recursive execution.

This thesis presents an ECG-based algorithm and method of execution that should assist physicians in quickly localizing the VTSO. This will be demonstrated through the results of our retrospective studies involving clinical data. A useful algorithm should be

simple, able to be integrated into current ablation protocols, provide near-real time results during a procedure, remain robust enough to correct for data variation among patients caused by their unique PM locations and scarring, and ultimately provide a unique and focused AoP for the VTSO. The algorithm and method presented hear satisfy all of these requirements and has the potential to significantly reduce the normal operating time of a standard VT ablation procedure thereby improving patient care while reducing costs.

Chapter 2 – Brief Review of Heart Physiology and Electrocardiography

In order to thoroughly understand the problem of ventricular tachycardia source of origin (VTSO) localization, it is important to have a basic understanding of the electrophysiology of the heart, how various arrhythmias can originate, and exactly how physicians treat these arrhythmias using cardiac ablation procedures.

2.1 – Heart Physiology

The heart consists of four chambers: the left and right ventricles, and the left and right atria. The right ventricle pumps blood to the lungs where it absorbs oxygen. Blood then returns to the left atrium, moves to the left ventricle, and is pumped to the rest of the body. The oxygen-depleted blood returns to the left atrium and the cycle repeats. An image depicting this circulation cycle is shown in Figure 2-1a. Additional anatomical labels are shown in Figure 2-1b.

The heart itself is enclosed within a double walled sac known as the pericardium. The inner layer of the pericardium is called the visceral pericardium, or epicardium. This is also the outermost of three layers making up the heart. The other two layers are the myocardium, consisting of contractile muscle, and the endocardium, which is in direct contact with the blood and merges into the endothelium. Scarring within these layers of heart tissue often leads to ventricular tachycardia (VT).

a.

b.
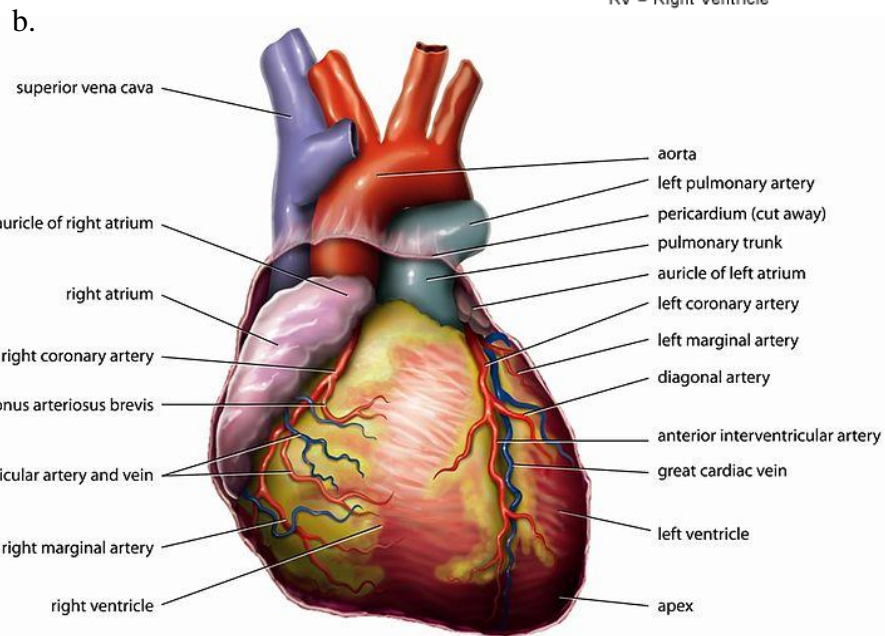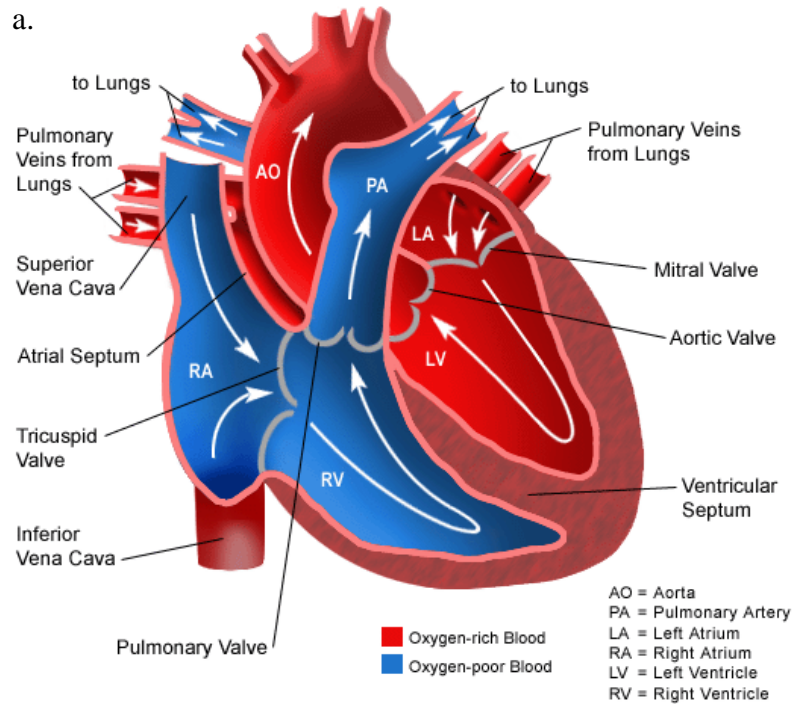
Figure 2-1. Circulation and anatomical diagrams of the heart.

2.2 – Anatomical Terminology

During medical procedures and within any medical source of information discussing the heart, anatomic locations of the heart are considered common knowledge.

These terms help surgeons to quickly communicate to others points of interest on or within the heart by identifying particular regions or surfaces. These terms are defined below for engineers less familiar with this medical terminology.

The common terms 'top' and 'bottom' are normally referred to as superior and inferior, respectively. 'Front' and 'back' are referred to as anterior and posterior, respectively. The base, or basal, portion of the heart is essentially the top portion of the heart. More specifically, it describes the region superior, posterior, and to the right (from the patient's perspective), mainly consisting of the left atrium and a portion of the back part of the right atrium. On the opposite end, the apex, or apical, region of the heart is the lowest part. More specifically, it describes the region inferior, anterior, and to the left.

In addition to the terms for the general directions of the heart, there are medical terms that help define the separations of the various chambers. On the exterior of the heart, the coronary sulcus is the groove circling the surface of the heart and separating the atria from the ventricles. Seen in Figure 2-2a, it contains a number of the large blood vessels of the heart including the right coronary artery and the coronary sinus. The term 'septum' is used to define the interior walls of the heart that separate the individual chambers. For example, the atroventricular septum is the septum separating the right atrium and left ventricle while the interventricular septum is the septum separating the two ventricles.

a.

b.
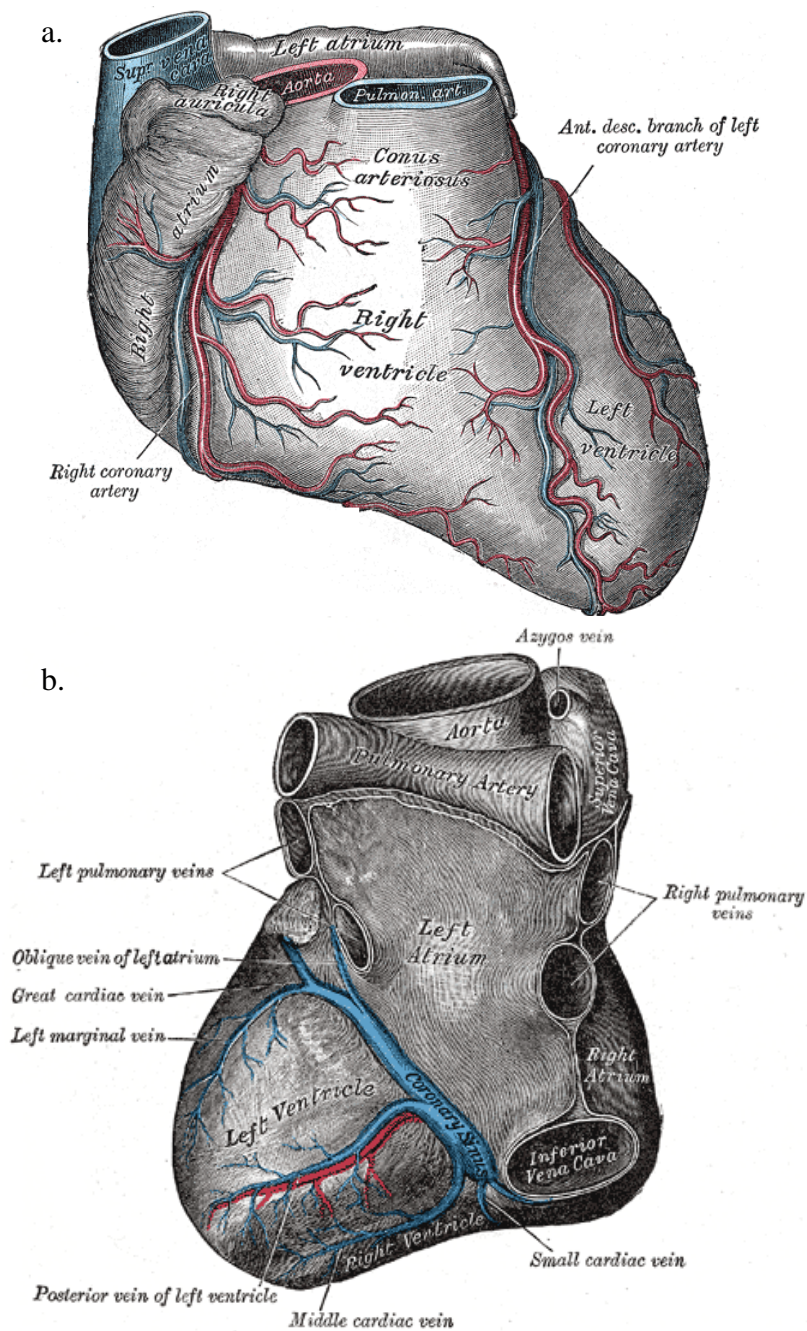
Figure 2-2. Sternocostal and diaphragmatic surfaces of the heart. The sternocostal surface (a.) consists of the right ventricle and right atrium, separated by the coronary sulcus. The diaphragmatic surface (bottom left of b.) and the base (top right of b.) are separated another segment of the coronary sulcus.

Shown in Figure 2-2 above, there are two main surfaces of the heart: the

sternocostal surface and the diaphragmatic surface. The sternocostal surface is directed

anteriorly, superiorly, and to the left. The lower portion of the sternocostal region

consists mainly of the right ventricle while the upper part consists of the right atrium,

separated from the lower region by the coronary sulcus. The diaphragmatic surface is

located inferiorly and slightly posteriorly. It is formed by the ventricles resting on the

diaphragm and is separated from the base by the posterior portion of the coronary sulcus.

2.3 – Cardiac Conduction Fundamentals

Properly coordinated systole (contraction) and diastole (relaxation) of the atria

and ventricles depends upon the complex electrical conduction system of the heart. This

coordination is achieved through a cyclic chain reaction of depolarization and

repolarization of the heart's myocardial cells. The sinoatrial (SA) node, often referred to

as the physiological pacemaker of the heart, begins the depolarization chain reaction. It

is a strip of specialized cardiac muscle approximately 3 mm wide and 15 mm long,

located in the superior posterolateral wall of the right atrium, as seen in Figure 2-3a [8].

Electrical signals spontaneously arise within the SA node at an individual's necessary

heart rate and stimulate nearby myocardial cells.

Myocardial cells have a naturally negative membrane potential. There is a higher

concentration of positive ions along the outside of the cell than immediately inside it -

i.e., the cell is polarized. When a cell is stimulated by the SA node, ion channels in the

cell membrane open allowing a rapid influx of Na^+ cations into the cell. This rapid

depolarization of the cell's charge balance causes additional channels to open, resulting

in a short influx of Ca^{2+} into the cell and an extended efflux of K^+ out of the cell. The

brief Ca^{2+} influx causes the cell to contract, while the extended K^+ release slowly

rebalances the charge difference, thereby repolarizing the cell and causing it to relax

again. The released K^+ also changes the polarity of nearby cells, causing them to open

their channels and depolarize. The result is a depolarization chain reaction in which a

wave of cells depolarizes, causing contraction, then repolarizes and relaxes.

The depolarization chain reaction, or action potential, travels faster along

specialized pathways within the heart, shown in Figure 2-3a. These pathways transmit

the action potential to localized groups of myocardial cells at specific times and are

responsible for the coordinated contractions of the atria and ventricles. Starting at the

SA-node, the action potential propagates to the left atrium via the Bachmann's bundle,

and to the right atrium via internodal tracts, stimulating both atria to contract in unison.

This pushes blood from each atrium into its respective ventricle. The action potentials

traveling along the internodal tracts aggregate at the atrioventricular (AV) node.
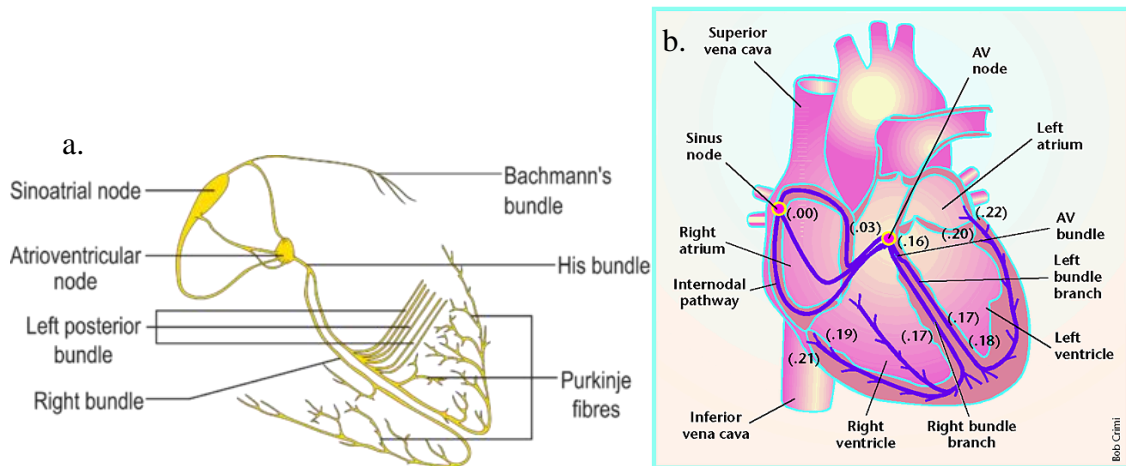
Figure 2-3. Electrical conduction system and timings (fractions of a second) of
an impulse through the heart [9].

The AV node is located in the posterior wall of the right atrium behind the

tricuspid valve. The AV node and its adjacent conductive fibers cause a delay in the

transmission of the action potential to the ventricles. This allows the atria to finish

emptying their contents into the ventricles before the onset of ventricular contraction.

10

The His bundle then splits the electrical pathway into left and right bundle branches, responsible for activating their respective ventricles. The Purkinje fibers transmit the signal to ventricular myocardial cells. These Purkinje fibers have a transmission rate approximately 150 times that of the AV node fibers and 6 times that of normal ventricular muscle, allowing for very rapid electrical transmission throughout the entirety of the ventricles after it passes through the AV node [8]. The rapid transmission reaches all ventricular myocardial cells within 0.06 seconds, allowing them to contract in unison. This provides a stronger contractile force to pump the blood to the rest of the body. The cardiac pumping cycle ends with first the atria, and then the ventricles depolarizing and relaxing. As the atria relax, they fill with blood and await the next SA node trigger.

It is important to note not only the pathway of the cardiac electrical impulse, but also the precise times of its appearance in the various parts of the heart. The conduction system and timings can be viewed in Figure 2-3b. A quantitative knowledge of the timing is necessary to attain a thorough understanding of electrocardiography because conduction speed influences the shape of the ECGs. If a heart contains a region of scarred or diseased tissue, conduction may be slowed in that region, resulting in inappropriate myocyte activation timing, potentially causing VT. This phenomenon is explained in further detail in Section 2-6. Electrocardiologists can spot slow conduction regions by observing abnormal localized ECG timing. However, it is necessary to have a basic understanding of electrocardiography before we get into the details of how the electrocardiologists perform this ECG analysis.

2.4 – Electrocardiography

The ECG records the electrical activity of the heart over time via skin electrodes. Exact ECG recordings thus rely on proper placement of these electrodes whose locations

are the right arm (RA), left arm (LA), right leg (RL), and left leg (LL), as well as the

points seen in Figure 2-4. In electrocardiography, the term 'lead' refers to a unique pair

of these electrodes. In this study, a normal 12 lead ECG configuration was utilized for

analysis. These 12 leads are I, II, III, aVR, aVL, aVF, V1, V2, V3, V4, V5, and V6.
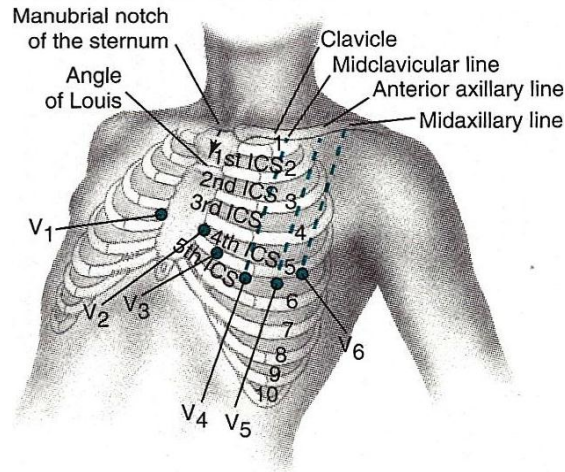
Figure 2-4. Placement of electrodes V1 through V6. This placement is used for a standard 12-lead ECG configuration.

Lead I refers to the potential between electrodes attached to the -RA and the +LA.

Lead II is between the -RA and +LL. Lead III measures the voltage between the -LA and

+LL. Einthoven's Law states that I + (-II) + III = 0. In addition to these three bipolar

limb leads, the three leads aVR, aVL, and aVF are known as augmented limb leads.

These are derived from I, II, and III, but view the heart from different angles. They each

utilize a modified negative input as shown in the following equations.

$$aVR = RA\text{-}(1/2)(LA+LL) \qquad\qquad \text{Equation 2-1}$$

$$aVL = LA\text{-}(1/2)(RA+LL) \qquad\qquad \text{Equation 2-2}$$

$$aVF = LL\text{-}(1/2)(RA+LA) \qquad\qquad \text{Equation 2-3}$$

The precordial leads (V1 through V6) are the difference between their respective

positive electrodes placed on the chest as shown in Figure 2-4, and Wilson's central

terminal, $V_W = (1/3)(RA+LA+LL)$, as the negative electrode. The precordial leads

vectorize the heart's electrical activity in the horizontal or transverse plane seen in

Figure 2-5. Combined with the coronal plane of the hexaxial reference system shown in

Figure 2-6, the physician can determine the direction of the electrical wavefront of the

heart simply by analyzing the 12 EKG leads. Furthermore, with both the transverse and

coronal planes of these depolarization vectors, the electrophysiologist has three

dimensional information on the electrical system of the heart. Therefore, during a cardiac

ablation (CA) procedure, an electrophysiologist can use the information from these 12

leads to help navigate toward the source of an electrical impulse, in this case the VTSO.

This classical method of locating the VTSO is discussed in more detail in Chapter 3.
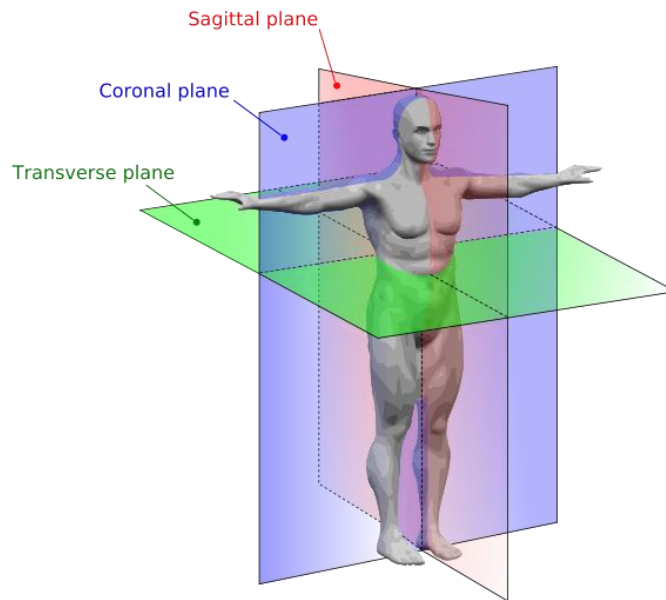
Figure 2-5. Planes of the body in anatomical position.

The 12 leads can be organized into subgroups which provide electrical

information on different regions of the heart. The inferior leads, including leads II, III,

and aVF, provide information on the conduction system of the diaphragmatic surface.

The lateral leads, including I, aVL, V5, and V6, provide information on the outside wall of the left ventricle. The septal leads, including V1 and V2, provide information on the electrical activity of the interventricular septum. The anterior leads, including V3 and V4, provide information on the electrical activity of the sternocostal surface of the heart. Chapter 3 includes more specifics on how electrophysiologists use the electrocardiograms from these leads to diagnose and localize the origins of tachycardias.
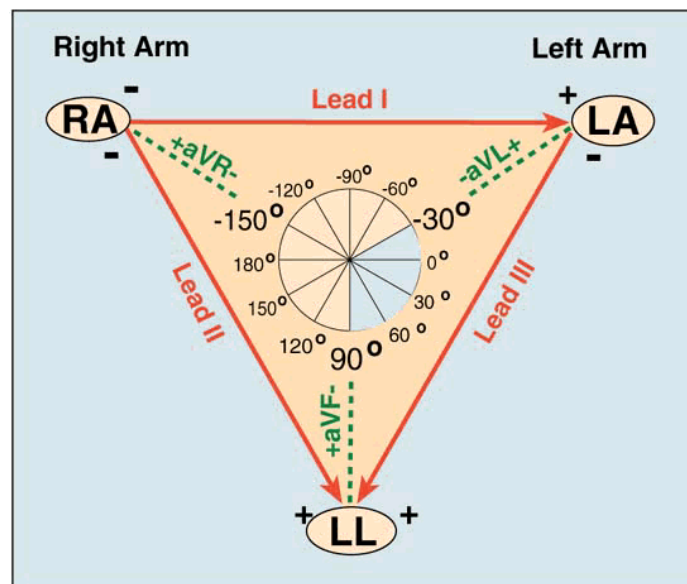
Figure 2-6. The hexaxial reference system and Einthoven's Triangle. This figure provides electrical information of the heart in the coronal plane (see Figure 2-5).

2.5 – The Electrocardiogram

A typical electrocardiogram (ECG) is shown in Figure 2-7 and includes a P wave, a QRS complex, a T wave, and a U wave some of which may be hard to discern on a particular ECG. The magnitudes of these waves are in reference to the baseline of the ECG, formally known as the isoelectric line. The R interval, or time between consecutive R peaks, is used to determine the heart rate. The P wave is a result of normal

atrial depolarization, during which time the electrical signal travels from the right to the left ventricle. The PR interval represents the time it takes for the electrical signal to travel from the sinus node, through the AV node, and on to the ventricles. The PR interval is used as a determinant of proper AV nodal function. The QRS complex represents the rapid depolarization of the left and right ventricles. The larger muscle mass of the ventricles correlates to the larger amplitude of the QRS complex when compared with the P wave. The T wave represents the repolarization of the ventricles. The QT interval extends from the beginning of the QRS to the beginning of the T wave. The baseline of the ECG is formally referred to as the isoelectric line. Specifics on how electrophysiologists normally use the ECG to locate the VTSO are detailed in Chapter 3.
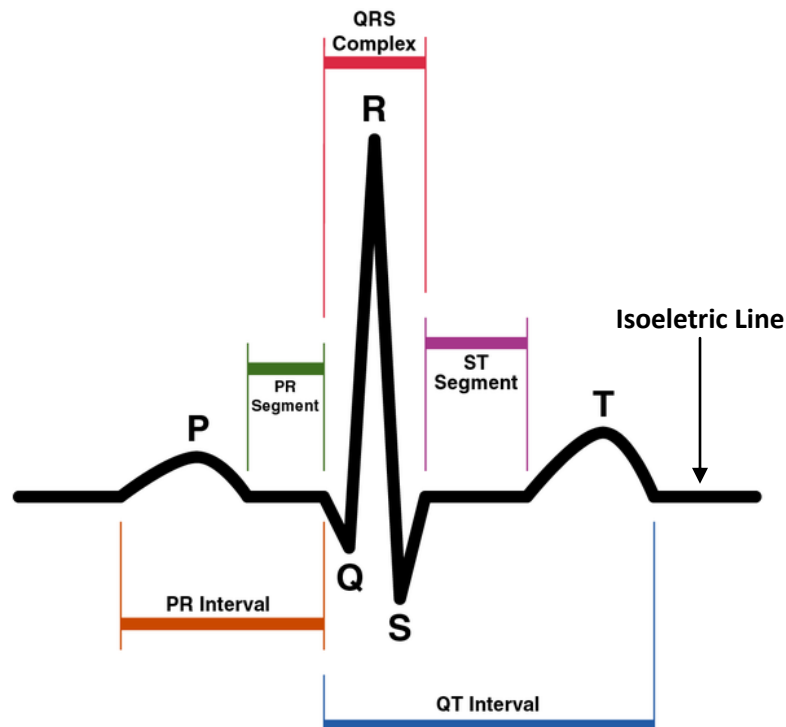
Figure 2-7. A typical ECG with labeled intervals. Used by electrophysiologists to diagnose and localize the sources of electrical conduction problems within the heart.

2.6 – Causes of Ventricular Tachycardia

In general, ventricular tachycardia (VT) is a fast heart rhythm originating in one of the ventricles. VT can lead to ventricular fibrillation, asystole, and sudden death. As seen in Table 2-1, a common mechanism of clinical ventricular tachycardia is reentry [10]. In reentry, a small portion of a ventricle's myocardial tissue conduct at a significantly slower rate than normal tissue. These small, often narrow regions are commonly surrounded and isolated from normal myocardium by anatomical blocking such as scar tissue from heart disease or even naturally occurring cardiac structures. These slowly conducting regions of tissue propagate the electrical signals during diastole instead of systole. Since these regions are narrow and frequently essential to the reentry circuit, it makes them ideal targets for ablation [10]. However, locating the exact location of these regions is another issue.

Once the excitation emerges from the slow conduction region, it creates a depolarizing wave emanating from the exit point. The depolarizing wavefront may then travel along the border of the scar, called the outer loop, or through the scar itself, known as the inner loop. Eventually, the electrical signal may reenter the slow conducting region, repeating the cycle. This cycle is in contrast to the normal cardiac cycle, and its self sufficiency is what causes the faster heart rate. To further complicate the matter, the reentrant circuit may have multiple entry and exit points. The purpose of cardiac ablation is to introduce small points of scar tissue that effectively disrupt the reentrant circuit returning normal sinus rhythm.

Table 2-1. Common mechanisms of various forms of VT [10].

VT Substrate Within a Small Region	Probable Mechanism
Idiopathic RVOT Tachycardia	(cAMP)-mediated triggered activity
Idiopathic LV Tachycardia	Infrafascicular reentry
Repetitive Monomorphic VT	(cAMP)-mediated triggered activity
Abnormal Automaticity	Enhanced Automaticity
Scar-related VT	Micro-reentry

VT Substrate Within a Broad Region	
Reentry Involving HPS	Macro-reentry
Bundle branch reentry	
Interfascicular reentry	
Scar-Related VT	
Prior myocardial infarction	Reentry, (automaticity)
ARVD	Reentry
Chagas' disease, sarcoidosis	Reentry
Repaired CHD	Reentry

2.7 – Cardiac Ablation

The term "radiofrequency cardiac ablation" is used to refer to the procedure in which a catheter inserted into the heart is used to directly apply high frequency alternating current to a focused region of heart tissue in order to disrupt the electrical connections of that region. Other types of ablation may use lower frequency AC or pulses of DC. As explained in Section 2.6, the target for ventricular tachycardias is often the region of slow conducting tissue contributing to a reentry circuit. By cutting off this slow conducting region, one essentially severs the reentry circuit, thereby preventing recurrent VT. However, the greatest challenge is not ablating the tissue itself, but identifying the exact location of the VT source of origin (VTSO) to ablate. A common method known as pace mapping as well as the latest experimental methods of locating this VTSO are explained in further detail in the Chapter 3.

Chapter 3 – State of the Art in VTSO Localization

As explained in Chapter 1, one of the common methods currently employed by electrophysiologists in localizing a VT is pacemapping (PM). However, there are many experimental methods that have been developed and are in development which aim to improve or assist the electrophysiologist to achieve a quick and accurate localization. An explanation of these methods along with their benefits and drawbacks is detailed in this chapter.

3.1 – Pacemapping

Pacemapping is a technique that involves stimulating, or pacing, myocardial tissue by injecting a periodic current pulse via cardiac catheter probe. These probes can be introduced either on the endocardial surface (typically via a femoral artery catheter) or on the epicardial surface via surgical incision. The pacing stimulation 'captures' the heart and overrides the normal pacemaker signals from the sinoatrial node. The electrical signals from the pacing can be measured using a standard 12-lead ECG [11]. The morphology of the 12 lead ECG is used for the comparison between the pacing site and the VT. At the origin of the VT, the QRS of the paced ECG should resemble the QRS of the VT ECG. The ECG resemblance of the paced QRS to the VT QRS has been shown to decrease as the pacing site gets further from the VTSO [14].

The electrophysiologist normally uses a commercial navigation system such as ESI or CARTO for the geometric data of the ventricles [12]. These sequential navigation systems (SNS's) store real time locations of the various catheters inserted into the ventricles. The SNS's help the electrophysiologist guide the catheters within the

ventricles by creating a ventricular surface model from the catheter coordinate data. Past pacing points are highlighted within and on the surface of the model.

It is important to note that pacemapping is largely a try and check method. The electrophysiologist paces at a site he hopes is the VTSO, checks if the PM ECG matches the clinical VT ECG recording, and then tries a new site if there is no match. An experienced electrophysiologist may form an educated guess as to the relative direction the VTSO is in from the last PM point, but it takes years of practice to become efficient. Pacemapping may require more than twenty pacing points and still fail to identify the VTSO.

3.2 – Voltage and Activation Mapping

If pacemapping does not immediately reveal the location of the VTSO, the electrophysiologist may switch to creating a voltage or activation map of the ventricle. To create these maps, a catheter is moved point-by-point along the endocardial surface, recording the endocardial electrograms from the catheter tip. The voltage magnitudes of these electrograms are color coded across the ventricle model, forming a voltage map. The timings of individual electrograms from the endocardial surface are compared with a stable reference electrode are color-coded on the surface model to create an activation map [11].

Low voltage regions on the voltage map often indicate regions of scar tissue. Since scar tissue is often the cause of a reentrant circuit, the maps help identify likely regions containing the VTSO. The activation map may indicate regions of slow conducting tissue, another important part of a reentrant circuit which leads to VT as described in Section 2.6. Although these two maps can help the electrophysiologist

identify the VTSO, the procedure involved in creating the maps is a separate process from pacemapping and takes additional hours to complete. Therefore, if an algorithm can efficiently and reliably locate the VTSO using only a few PM points, it will prevent the patient from having to undergo the separate time-consuming process of creating voltage and activation maps.

3.3 – ECG Characteristic Analysis

With the VT QRS morphology alone, electrophysiologists may be able to regionalize the location of the VTSO or exit site. The features of the ECG that are focused on include the QRS width, the QRS axis, the concordance, and the presence of QR complexes [13]. The width of the QRS helps determine whether the site of origin lies on the free wall or on the septum. Septal VTs have a narrow QRS while sites of origin on the free wall have a wider QRS.

Concordance means that the QRS of the precordial leads (V1-V6) are either all positive or all negative.   Positive concordance (i.e. all V leads are positive) indicates a VT originating in the base of the heart. On the other hand, negative concordance occurs in VTs originating in the apical septum [13]. A QS complex is a QRS wave without a positive component and indicates that the VTSO is causing activation to move away from the site recording the QS. For example, QS complexes in inferior leads indicate an origin located on the inferior wall, and QS complexes in the precordial leads indicate an origin on the anterior wall [13].

The hexaxial reference system from Figure 2-6 can also be used to help identify the origin of a VT. A right superior axis VT (VT wavefront in the range of -90° to -150°) indicates an origin in the septal or lateral regions of the apex. Left inferior axis VTs (VT

wavefronts in the range of 30° to 90°) suggest an origin in the superior right free wall or possibly the top left interventricular septum.

As shown in Figure 2-2, after the electrical impulse passes through the His bundle, it splits into a right bundle and left bundle of conductive pathways. If the right or left bundles become injured due to some form of heart disease or infarction, they may stop conducting electrical impulses correctly. This is known as right bundle branch block (RBBB) and left bundle branch block (LBBB), respectively. These blocks result in ECG patterns shown in Figure 3-1, which may be used to help identify the VTSO. A left bundle branch block (LBBB) pattern indicates a VTSO in either the right ventricle or possibly the left side of the interventricular septum. In contrast, right bundle branch block (RBBB) patterns usually indicate a VT arising from the left ventricle [13].
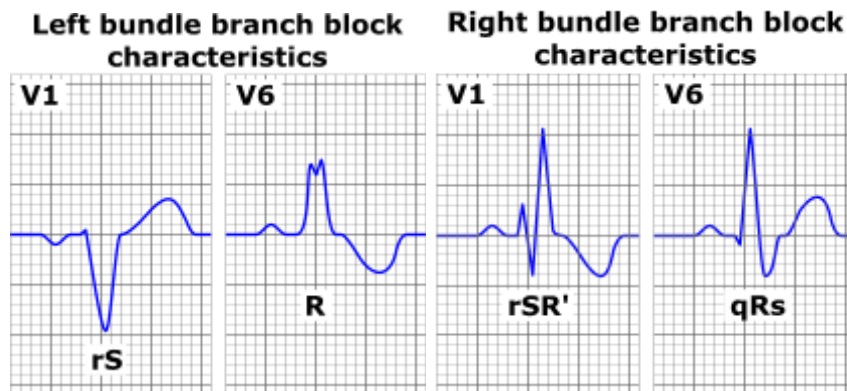
Figure 3-1. Left and right bundle branch block patterns. LBBB and RBBB are determined from ECG morphologies in the V1 and V6 leads. They help regionalize the origin of a VT to either the left ventricle or the right ventricle.

3.4 – Manual VTSO Regionalization Based on ECG Morphology

Algorithms have been designed to use the ECG morphologies described above in order to regionalize the exit site of a reentry circuit [4, 5, 6, 7]. Specifically, Segal et al. used the following ECG characteristics: LBBB and RBBB appearances, QRS polarity

(lying mainly above or below the isoelectric line, otherwise known as the base line) in the inferior leads, QRS polarity in leads I, aVL, and aVR, and R-wave transition (the precordial lead in which the QRS complex reversed) [4]. Their decision tree algorithm started with either RBBB or LBBB with following branches for the morphologies of the various leads. The algorithm ultimately assigned the VTSO to one of 9 regions: antero-apical, antero-basal, mid-anterior, apical-septum, basal-septum, mid-septum, posterior apex, postero-basal, and mid-posterior. These regions can be seen in Figure 3-2 below. The algorithm was able to regionalize the VTSO for 88% of the VTs studied and did so accurately for 84.3% ± 4.9% of those VTSOs [4].
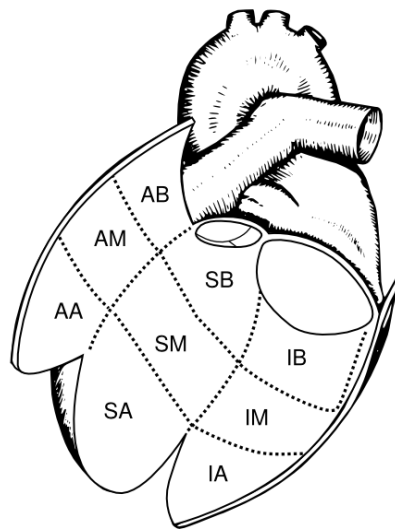
Figure 3-2. Division of the ventricle into 9 regions. The labels are defined as: AA= antero-apical; AB = antero-basal; AM = mid-anterior; SA = apical septum; SB = basal-septum; SM = mid-septum; IA = inferior apex; IB = inferior-basal; IM = mid-inferior. Image courtesy of Dr. Jonas de Jong and ECGpedia.org.

Ito et al. also developed a decision tree algorithm based on ECG morphologies for the purpose of regionalizing potential ablation sites for VTs [5]. The ECG characteristics used in this algorithm were the presence/absence of an S wave in lead V6, the magnitude and width of the R wave or QS complex in leads I, V1, V2, aVR, and aVL, the QRS

morphology in leads I, II, III, aVL, and aVF, and R-wave transition. This algorithm

localized the origin to one of six regions: the LV endocardium, LV epicardium, left sinus

valsalva, RV septum, RV free wall, and near the His bundle (see Figure 2-2). This

method, while used only for idiopathic ventricular outflow tract tachycardias, had an

accuracy of 88% [5].

While these regionalization methods do show some promise, there are a few

drawbacks to their clinical use. First, the regions are large, implying poor localization

resolution. While regionalization does help the electrophysiologist narrow down his

search for the VTSO, it typically needs to be augmented by pacemapping to provide

sufficient final resolution. Furthermore, the regionalization process is not automated,

adding to the analysis time and introducing potential human error.

3.5 – Automatic Regionalization of VTSOs

Sanroman-Junquera et. al. attempted to automate the regionalization method using

neural networks trained with patients' ECG data that had been stored in their implantable

defibrillators. This method divides the ventricle into three pairs of halves, forming eight

octants. The neural networks analyze the morphologies of the ECGs, using the

amplitudes of key deflections in each channel to create a voltage map. This voltage map

is plotted on the surface of a three dimensional CARTO recorded model of the ventricle

in question. Based on the voltage map, the VTSO is assigned to one of the octants.

While this method creates a unique map for each patient, it ultimately assigns the origin

to a predefined region like the previously described algorithms. Furthermore, while this

system is automated, the accuracy for regionalizing the VTs to their actual octant has an

accuracy of only 36.3%. Improvements in both the accuracy as well as in focusing down the size of the likely location of the VTSO can and should be made.

3.6 – Noninvasive localization Methods

Zhang et al. use a body surface potential map combined with a CT scan of the ventricle to create a three dimensional activation map throughout the ventricle's myocardium, not just the epicardium or endocardium [7]. The error in localizing sites of activation is approximately 5.73 mm ± 1.77 mm and the activation times were within approximately 5.5 ms of the actual activation times. This procedure shows great promise in that it is noninvasive, meaning it does not involve inserting a catheter into the heart and pacing. This would significantly reduce the stress on the heart. It also gives the electrophysiologist a view into the internal electrophysiology of the myocardium, whereas he normally only has access to the internal and external surfaces. This gives him a better idea of how abnormalities such as internal scar tissue are affecting the electrical circuitry of the ventricles.

However, this procedure does require an entirely new procedure that is not easily integrated into the current method of pacemapping and ablation procedures. A CT scan of the ventricle must be acquired prior to mapping. Additional body surface potential mapping requires anywhere from 40 to 60 electrodes placed in an array on the torso [7]. The additional time, equipment, and procedures would take years or decades to successfully integrate into standard clinical practice for ablation procedures. A faster, more easily integratable alternative would be ideal.

Chapter 4 – The ECG Inverse Problem Regarding VTSO Triangulation

4.1 – The ECG inverse problem

In electrocardiography, the ECG inverse problem refers to deriving regional information about the electrical activity within the heart using only electrical measurements on the body surface, i.e. ECGs. The desired regional information may include activation maps which provide location and amplitudes of activation wavefronts or extremums, or it may include the site of origin of ventricular tachycardia (VTSO). In this thesis, the focus is on the VTSO. Specifically, this research aimed to develop and test an automated method that can use body surface ECG recordings acquired during pacemapping to provide a clinically useful target region containing the VTSO with reliability, speed, and ease of use.

A 'clinically useful' target region is defined as a region small enough to allow the electrophysiologist to ablate the VTSO with a single "burn". For example, splitting the heart into various regions such as apical-septum, basal-septum and mid-septum, and then assigning the VTSO to one of these regions after ECG analysis is not considered clinically useful since the electrophysiologist cannot ablate the entire apical-septum region of the ventricle. Although using a large target region, such as half the surface area of the ventricle, may be mathematically accurate in that it correctly contains the VTSO across various patients and circumstances, the size of the region is not particularly useful to the electrophysiologist. The electrophysiologist would only know that the VTSO is located somewhere on that particular half of the ventricle and nothing more.

'Reliability' is defined as the ability to provide an accurate solution while operating with measurement noise, geometric modeling errors, and other potential issues that are common in clinical practice. For real-time applications, rough geometric models will be created and used when accurate geometric measurements of the ventricle in question are unavailable. If a method cannot operate accurately without the use of precise geometric data, its clinical utility is reduced.

'Speed' refers to the procedural time in pinpointing the VTSO location. Normal cardiac ablation procedures may take hours and tens of pacemapping (PM) point recordings followed by additional hours of voltage or activation map creation before the VTSO is finally located. Accurately localizing the VTSO using only a few PM points would significantly reduce operation time. Therefore, a fast method must use a reduced number of PM points compared to normal procedures in order to reduce total operation time.

'Ease of use' is defined as mostly automated and easily integratable into the current cardiac ablation procedures. Automated refers to requiring minimal input from the operator in order to derive a solution. Furthermore, if the method is too complex, operation time may increase and adoption of the system into clinical practice may become less likely. To the best of our knowledge, we believe we have created the first method that solves the inverse problem in regard to VTSO localization which satisfies all of these conditions.

4.2 – Analysis of State of the Art in VTSO Localization

As explained in section 3.2, ECG morphology analysis is commonly used by electrophysiologists during normal cardiac ablation procedures in regionalizing the

VTSO. However, this is not an automated method; instead it requires the full attention and experience of the electrophysiologist. It also does not provide very high resolution, assigning the VTSO to one of several large regions of the heart.

Section 3.3 explained how Segal et al. and Ito et al. attempted to automate ECG morphology analysis with the use of a decision tree, reducing the mental strain on the electrophysiologist with step-by-step morphological checks [4]. However, this approach failed to address the limited resolution of the classical approach and thus failed to provide a significant advance.

As explained in Section 3.4, Sanroman-Junquera et al. attempted to further automate the process using neural networks that analyze stored ECGs and provide a higher resolution solution for VTSO location. However, the method ultimately assigned the VTSO to a ventricle octant and did so with an accuracy of only 36.3%. Therefore, this method still has significant issues with accuracy and reliability as defined in Section 4.1.

I have also explained how Zhang et al. attempted to create a noninvasive, automated method for creating activation maps that provide useful geometric information in locating VTSOs. However, his method depends on the use of a CT scan and a body surface potential map which are necessary for this method and which reduce the ease of use of this system. The components are complex and costly, making it difficult to integrate into current cardiac ablation practice.

While each of the published algorithms and methods described in this section has some useful features, none of them satisfy all of the requirements for the problem solution outlined in Section 4.1.

4.3 – Potential Impact of a Solution

The benefits of a solution satisfying the previously explained requirements are both diverse and significant. First, the solution will significantly reduce cardiac ablation operation time, since a large portion of the total procedure is dedicated to pacemapping and localizing the VTSO. Second, the reduced procedure time will reduce the physical stress on the patient which may in turn reduce complications caused by extensive pacemapping. Third, the reduced procedure time reduces the man-hours, anesthesia, and other medical supplies used per operation, significantly reducing the hospital cost per procedure. Fourth, this savings may extend to the patients, allowing those in a lower economic class to receive the procedure who otherwise could not afford it. Shorter procedures also free up time for easier patient scheduling. Fifth, the automated method reduces the mental strain on the electrophysiologist who must already keep track of numerous sources of real-time information. This allows him to focus more on the patient, potentially preventing human errors and catching unforeseen complications before they occur.

One other potential benefit comes directly from the method's ease of use. Practicing electrophysiologists must undergo years of specialized training, residency, and supervised clinical practice before they become familiar with the method of navigating to the VTSO based on PM ECGs. The automated method may assist electrophysiologists, both in training and early practice, to become more familiar and confident in quickly navigating to the VTSO.

These benefits are compounded when considering that over the past decade, cardiac ablation procedure rates have been increasing [15]. This suggests larger throughputs of patients, larger totals of hospital time dedicated to these procedures, and larger numbers of electrophysiologists trained in cardiac ablation. The method presented in this paper may help to mitigate some of these emerging national issues.

Chapter 5 - Methodology

In order to develop the VTSO triangulation method described in Section 4.2, ECG data were acquired from patients at the University of Maryland Medical Center in Baltimore who underwent cardiac ablation VT procedures. All patients provided prior consent for releasing their ECG information for research purposes (see Appendix A for a chart of the patients involved in the study). The ECG data were captured using a standard 12 lead configuration (see Section 2.2 for body surface lead placement). Catheter pacing was applied to the endocardial ventricular wall at localized PM points using 400 ms cycle length and 2.0 ms pulse duration. The ECG data were digitally recorded using either Prucka Cardiolab software (General Electric, Fairfield, CT) after a band pass filter was applied (0.05 – 100 Hz) or NavXVelocity Packet Capture Software (St. Jude Medica, Inc., St. Paul, MN) with the data in its unfiltered form.

The custom VTSO navigation software was developed and programmed using MATLAB R2009a software (The MathWorks, Inc., Natick, MA). MATLAB provides built in, high level functions for signal and data analysis as well as a robust Graphic User Interface (GUI) creator. The GUI creator is important because the VTSO navigation algorithm requires significant user input concerning data selection and data conditioning.

More specifically, the VTSO navigation algorithm that was developed is based upon a correlation between the difference in ECG morphology of two PM points, or a PM point and the VT, and the distance between the two points. A signal difference – distance linear correlation is made using three PM points located at arbitrary positions on the endocardial surface of a ventricle. This correlation line is then used, along with the clinical VT ECG, to determine the distance between the VTSO and each PM point. The

overlap of the regions defined by those three distances defines a target region of the ventricular surface that is expected to contain the VTSO. One could use the analogy of cell phone triangulation, with three cell phone towers representing the PM points, the cell phone representing the VTSO, and the signal strength representing the ECG signal differences. Details concerning the development and testing of the VTSO navigation algorithm are described in the following sections.

5.1 – Acquisition of VT ECG Template

The VTSO navigation algorithm is based upon the observation that the closer a PM point is to the VTSO, the more the PM ECG resembles that of the clinical VT [14]. Therefore, the first piece of data necessary for the functioning of the VTSO navigation algorithm is a clinical VT ECG template to use as a reference. This template is acquired in one of two ways. The VT ECG template can be recorded before the procedure begins if the patient is naturally presenting VT. If this is not the case, then the electrophysiologist can stimulate the ventricles into a temporary state of VT at the beginning of the CA procedure. The VT is induced by applying a pacing train at specific frequencies and power levels. The electrophysiologist in charge of the case is trained in methods of safely inducing the VT, which requires unique adjustments based on each patient's response to the stimuli. The ECG data is captured using a standard 12 lead configuration (see Section 2.2 for body surface lead placement). Once a few seconds of VT ECG information is recorded, the ventricle is paced again and brought back into normal sinus rhythm. Now that the VT ECG template is digitally recorded, the next step is to acquire pace mapping points.

5.2 – Acquisition of Three PM Points

After the VT ECG template is acquired, the electrophysiologist begins the pace mapping process as described in Section 3.1. The electrophysiologist paces at three arbitrarily selected locations on the endocardial surface of the ventricle, digitally recording the ECGs at 1200 samples per second. These three pace mapping (PM) points will ultimately be used to triangulate a target region of the ventricle that contains the VTSO. Details on the pacing and recording settings are found at the beginning of Chapter 5.

In addition to the 12-lead ECG information, the geometric location of the catheter tip before, during, and after pacing is recorded in Euclidian coordinates (mm). All of the geometric data together is used to create a surface model discussed in more detail in Section 5.8.2. Considering each particular PM points, we now have an associated 12-lead ECG and an (x, y, z) coordinate defining where the pacing took place on the endocardial surface. Using the ECGs and locations of these three PM points, we can perform signal analysis to quantify the relationship between the ECG signal similarity of two PM points and the distance between those two points. However, we first need to extract out a single QRS segment of each PM ECG. To facilitate signal analysis, the signals must all be the same size and represent the QRS region of each particular PM point.

5.3 – Identification of the QRS region for PM points

Catheter pacing within the heart is normally observable as an artifact in all of the 12 channels of a recorded ECG. An example of a pacing artifact for a single ECG channel can be seen in Figure 5-1. In these cases, selection of the QRS segment used for

signal analysis is usually straightforward because the artifact and the QRS segment are
separate, distinct, and easily identifiable.
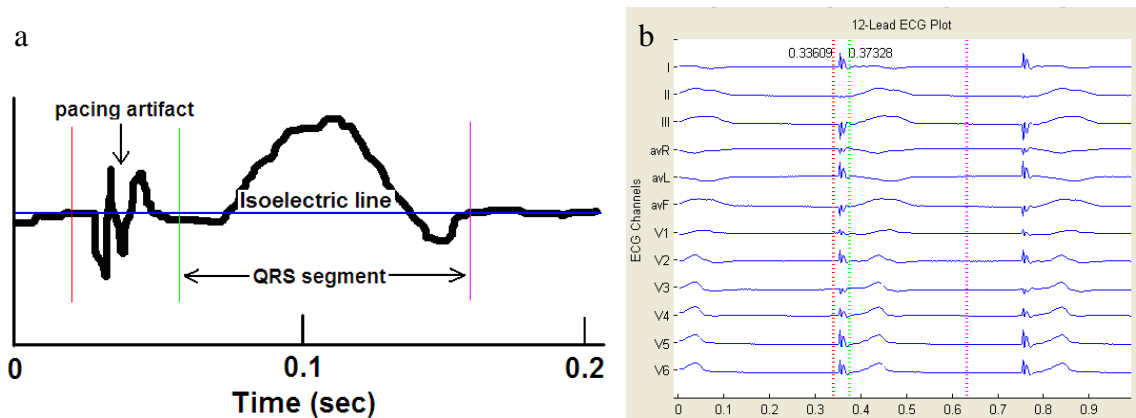
Figure 5-1. Single channel pacing event (a) and 12 channel ECG for a
single PM point (b).

After pressing a marker button, the user is able to mark the beginning of the QRS
region by selecting a point immediately after the pacing artifact. An example of an ideal
location is the solid green line in Figure 5-1a. The user must then select a reference
voltage value to be used as the isoelectric line, or baseline, of each channel ECG. This is
also manually selected by the user by placing a red marker at the time immediately before
the pacing spike. The voltage of the ECG at the marked time is set as a 0 V reference for
the channel, forming the isoelectric line (Figure 5-1a). The end of the QRS region is
indirectly input by the user via specifying the total number of data points. The total
number of data points refers to the number of data points making up the QRS region.
Assuming data is obtained at 1200 Hz, this number will be in the range of 150 to 250.
Once entered, a line indicating the end of the QRS region is automatically drawn at a
location the given number of data points away from the green QRS start line, indicated by
the purple marker in Figure 5-1 a. Because all 12 channels for a pacing point are plotted

together, setting these markers keeps all QRS segments for all channels the same length as shown in Figure 5-1b, facilitating the ECG analysis portion of the program.

By specifying the number of data points and changing the start of the QRS line, the user also has the ability to base the analysis on a subsection of the QRS region, such as the first third. This allows the user to perform additional studies based on different ECG sections.

5.4 – Automatic Identification of the QRS Region of VT Template

Selection of the QRS region becomes a more difficult problem when there is no pacing artifact as for a VT ECG seen in Figure 5-2. Without the pacing artifact as a reference, it becomes very difficult to determine the start of the QRS region. I have designed a simple algorithm that can be used to help automate this selection process.
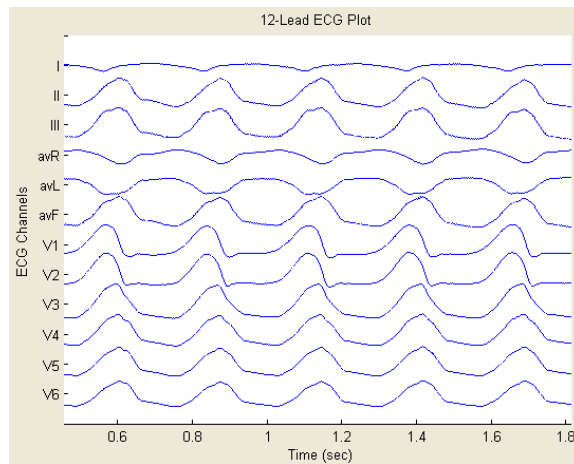
Figure 5-2. VT ECG without pacing artifacts. It is difficult to determine where the QRS region begins and ends in ECGs such as this one. This data is from patient 2.

The algorithm is based on a cross-correlation sum function. Cross-correlation is a measurement of waveform similarity between two signals as a function of time lag applied to one of the signals. It is important to note that unlike the convolution of two

33

waveforms which reverses a signal before shifting and multiplying it, the cross-correlation only involves shifting and multiplying. The definition of the cross-correlation function used is given as Equation 5-1 with an output vector c given by $c(m) = R_{xy}(m-N)$, m=1, ..., 2N−1 where x and y are the two ECG waveforms, N is the maximum lag, or twice the length of the x and y waveforms, and m is a specific lag value.

$$\hat{R}xy(m) = \begin{cases} \sum_{n=0}^{N-m-1} x_{n+m}y_n^* & m \geq 0 \\ \hat{R}yx^*(-m) & m < 0 \end{cases}$$

Eq. 5-1

The cross-correlation is applied to each individual channel of the VT and the corresponding channel of a PM point. The output vector for each channel cross-correlation is normalized by dividing through the peak value so the max value in each output vector is 1.0. The cross-correlation vectors are then summed for all 12 channels. The lag at the peak value (absolute value) of this summed cross-correlation is used to define the start of the QRS region for the VT ECG data.

The absolute value is used because the QRS region can appear above or below the isoelectric line. If VT QRS regions are positive (above the isoelectric line) in most channels, like those seen in Figure 5-3a, and negative for most channels in a PM ECG (Figure 5-3b), the maximum positive value in the cross-correlation sum plot (Figure 5-3c) would identify a flat ECG region as the likely QRS segment (Figure 5-3d). This region selection is made because a flat line cross-correlated with a negative QRS gives a more positive result (even if that result is 0) than a positive QRS cross correlated with a negative QRS. Using the absolute value (Figure 5-3e) corrects this problem, correctly identifying the VT QRS region (Figure 5-3f). The complete code for automated QRS selection based on cross-correlation sum is shown in Appendix B-1.
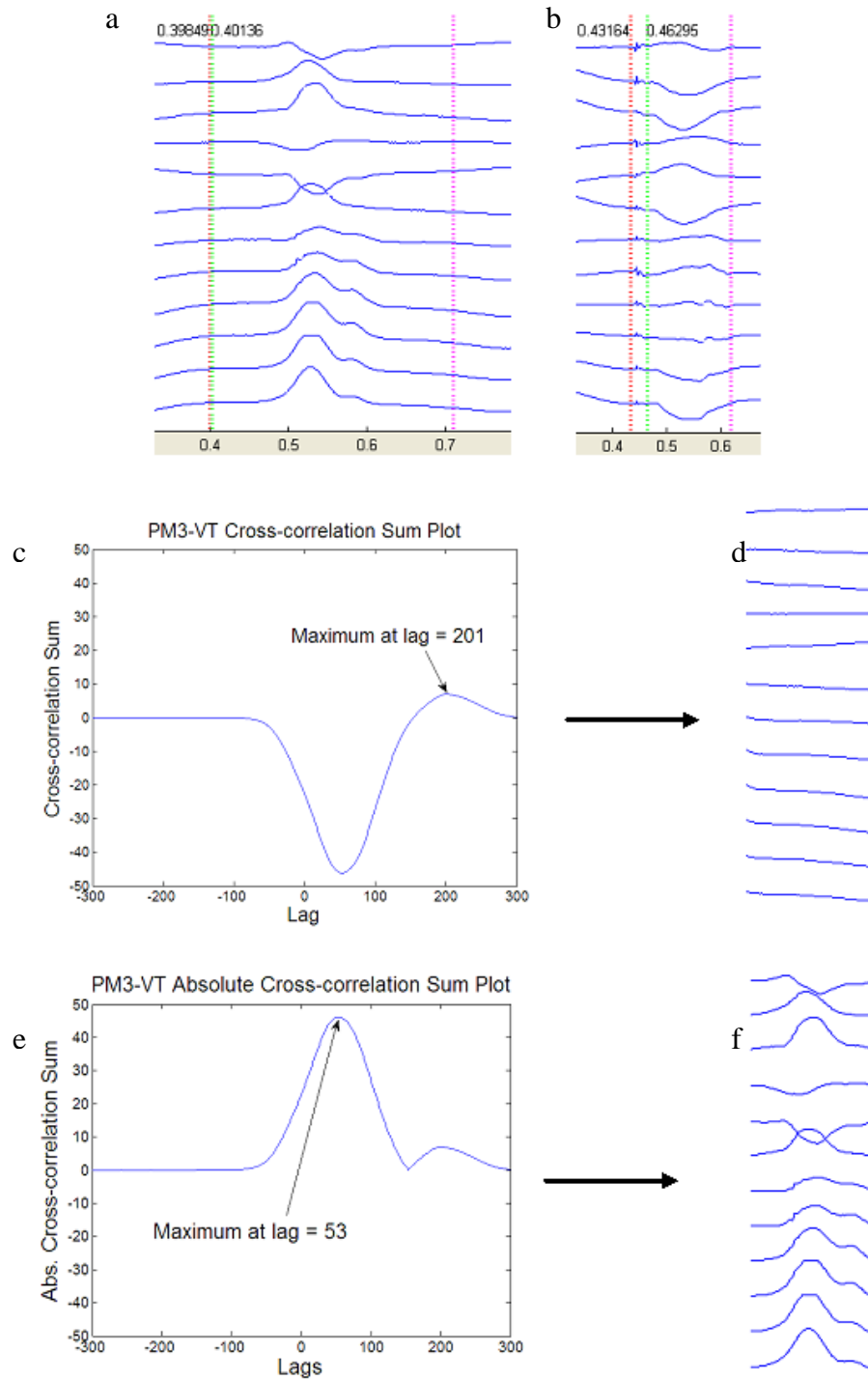
Figure 5-3. Cross-correlation sum algorithm with and without absolute value. The VT ECG channels (a) are cross correlated with the PM ECG channels (b). The resultant is summed creating plot c and the absolute value of the plot forms e. Using the peaks from c and e results in extractions of signals d and f, respectively.

5.5 – Selection of ECG Analysis Metric

With the QRS segments selected from the recorded ECGs, signal analysis can now be performed. The main principle behind the VTSO navigation algorithm is the idea that the closer together two PM points are, the more similar their respective ECGs become. This relationship is also true for a VT and a pacing point. Pacing at the VTSO produces an ECG closely identical to the clinical VT. Based on this logic, there should be a correlation for the distance between PM points and the difference in their ECG signals. The metric used for calculating this difference in ECG signals would therefore have a large impact on the correlation and the overall effectiveness of the VTSO navigation program. The four main metrics analyzed include the sum of the root mean square error for each lead (RMSE sum), the mean absolute difference (MAD), the correlation between two ECGs (Corr), and the covariance (Cov). These four ECG metrics were plotted against distance for each unique pair of PM points for each patient. Comparison of the correlation coefficient (R) for multiple patients indicated that the RMSE Sum consistently provided the best result for distance vs. ECG metric plots, as seen in Table 5-1. Among the tested metrics, the RMSE Sum calculation provided the largest mean and median R values and the lowest standard deviation, identifying it as the best metric suitable for the VTSO navigation algorithm.

An example of a metric comparison plot can be seen in Figure 5-4 below, comparing all four metrics for the same PM points and the same patient. Each point on the plots represents the metric vs. Euclidian distance for a unique pair of PM points.

Table 5-1. ECG analysis metric comparison chart. The R values represent the correlation between the given ECG metric and Euclidian distance between unique PM point pairs. The mean, median, and standard deviations suggest that the RMSE Sum is the best choice in creating a predictive model.

Patient #	# PM points	LV or RV	Correlation Coefficient (R)			
			RMSE Sum	Corr	MAD	Cov
1a	16	RV	0.9032	-0.8267	0.8907	-0.7642
1b	15	LV	0.7925	-0.7805	0.8283	-0.6699
2	7	LV	0.8254	-0.8569	0.7963	-0.7838
3	7	LV	0.9033	-0.8896	0.9094	-0.9069
4a	8	RV	0.9083	-0.8513	0.8699	-0.8068
4b	5	LV	0.8724	-0.7800	0.8608	-0.8037
5	9	LV	0.7918	-0.5556	0.6942	-0.5497
6	8	LV	0.8570	-0.8353	0.8560	-0.8324
7	7	LV	0.8533	-0.8351	0.8860	-0.7644
9	7	LV	0.9779	-0.8419	-0.8934	-0.7571
10	23	LV	0.6855	-0.6700	0.7452	-0.6858
11b	4	LV	0.7526	-0.5561	0.7420	-0.5842
12	10	LV	0.7661	-0.6562	0.7590	-0.6382
13	6	RV	0.8621	-0.7018	0.8493	-0.5324
14	11	RV	0.9444	-0.8792	0.9352	-0.8647
15a	13	RV	0.6838	-0.7047	0.7131	-0.5473
15b	21	LV	0.4964	-0.5190	0.5933	-0.5166
		Mean:	0.8162	-0.7494	0.7080	-0.7063
		Std. Dev.:	0.1170	0.1217	0.4223	0.1259
		Median:	0.8533	-0.7805	0.8283	-0.7571
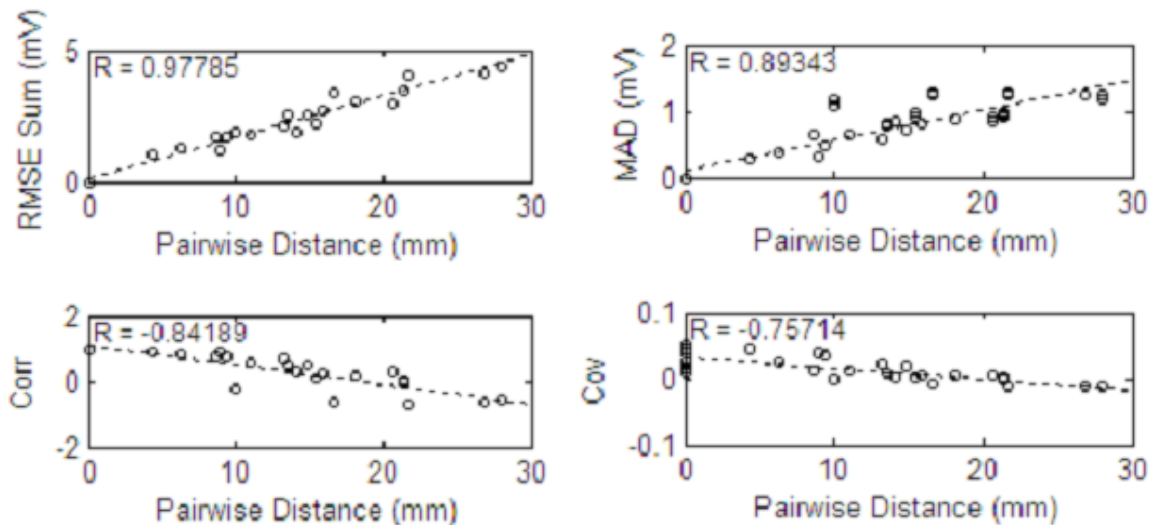
Figure 5-4. Metric comparison plot. The data provided is from patient #9. Each point on the plot represents ECG metric analysis vs. distance for two unique PM points. A larger absolute R value suggests a better predictive model.

The RMSE Sum is calculated from a QRS segment in all 12 ECG channels for a pair of PM points (or a PM point and the VT) and is represented by Equation 5-2,

$$RMSEsum = \sum_{i=1}^{12} \sqrt{\frac{1}{n} \sum_{j=1}^{n} (V1_{i,j} - V2_{i,j})^2} \qquad \textbf{Eq. 5-2}$$

where i represents one of the twelve channels for an ECG recording, j represents a single recorded time point, and n represents the total number of time points for a single channel ECG. $V1_{i,j}$ and $V2_{i,j}$ represent the voltages of two PM points at corresponding time points. The voltage magnitudes are with respect to the isoelectric line of each channel. Refer back to Sections 5-3 and 5-4 for details on how the isoeletric line and the individual QRS segments are selected. The code for calculating the RMSE Sum is provided in Appendix B-2.

5.6 – Selection of Distance Metric

Initial RMSE Sum-distance correlations relied upon Euclidian distance calculations between the XYZ coordinates of the PM points. However, this method suffered from a major limitation concerning the transmission of electrical signals within the heart. Cardiac neurons, including those making up the Purkinje system of the ventricles, are only present within the hear tissue. These signals are communicated between adjacent cells and cannot jump across the ventricular chamber. Therefore, using a distance formula such as Euclidian distance between PM points on opposite sides of a ventricle may be inappropriate as it does not follow the expected signal transduction path. Figure 5-5 shows how Euclidian distance can cause correlation issues. Using PM points from locations on all sides of the ventricle resulted in a relatively poor correlation with an

R of 0.39932 while using a subset of points on one side of the ventricle resulted in an R of 0.76892, which is a significant improvement.

a

b
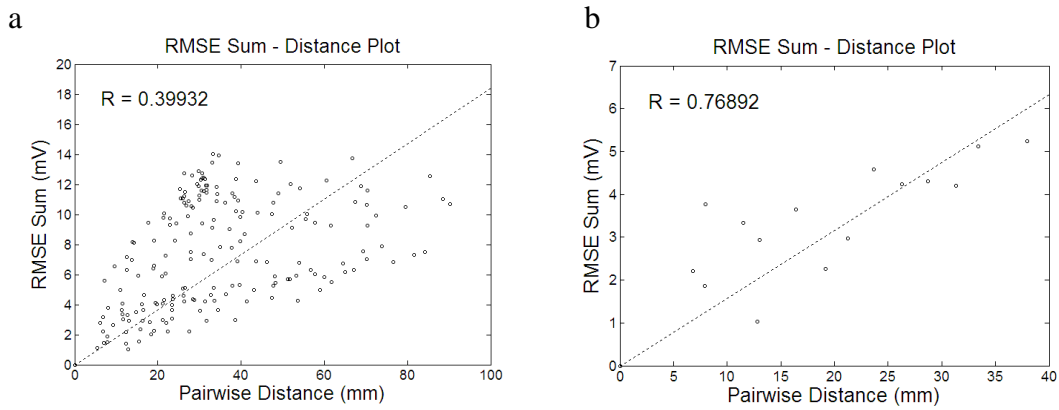
Figure 5-5. RMSE Sum – Distance plots using the full set (a) and subset (b) of PM points for Patient 15 b. The R value was calculated from the least squares linear regression constrained through the origin.

It became apparent that in order to improve the correlation for points on all sides of the ventricle, we needed a distance algorithm that computed the shortest distance between two points along the surface of the ventricle. The following algorithm was developed to approximate this surface distance.

The midpoint of the Euclidian distance between the two PM points (PM1 and PM2) is calculated. The midpoint's nearest neighbor on the surface is then determined (SP1). The new distance is then computed as the sum of the Euclidian distances between PM1-SP1 and SP1-PM2. The algorithm can be recursively called using the point pairs PM1-SP1 and SP1-PM2. Increasing the number of recursions improves the accuracy of the surface distance approximation, but also increases computation time. Figure 5-6 illustrates the principle behind the surface distance algorithm when used with a 2D set of data. The actual method is extended into the third dimension.
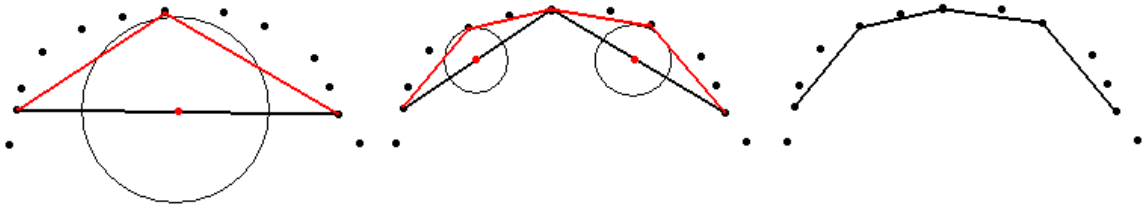
Figure 5-6. Two iterations of the surface distance algorithm. The steps are in order from left to right. The black lines represent the current Euclidian distances with the red dots indicating their midpoints. The circle simply shows how the nearest neighbor to the midpoint was identified. The red lines are the new Euclidian distances for additional recursions. The sum of the Euclidian distances represents the surface distance, as shown in the final step.

The surface distance approximation method provided some minor improvements over the Euclidian distance as seen in Table 5-2. However, the change in correlation was not considered significant for most patients. Since Euclidian distance gave similar results with a faster computation time, Euclidian distance was used in most additional data analysis. However, the surface distance makes more theoretical sense than the Euclidian distance and should be used in future versions of the program.

Table 5-2. Euclidian vs. surface distance comparison chart. The R values represent the correlation coefficient between the RMSE Sum and distance between unique PM point pairs. The mean R values suggest that surface distance may be the better choice in creating a predictive model.

			Corr. Coeff. (R)	
Patient #	# PM points	LV or RV	Euclidian	Surface
4a	8	RV	0.9083	0.8463
4b	5	LV	0.8724	0.9239
9	7	LV	0.9779	0.9702
11b	4	LV	0.7526	0.7740
13	6	RV	0.8621	0.7899
15b	21	LV	0.4964	0.5893
		Mean:	0.8116	0.8156

5.7 – RMSE Sum–Distance Data Modeling and Offset

With the RMSE Sum and distance metrics selected and applied to the three PM points of a patient, the data needed to be modeled. With a linear model defining the

relationship between the RMSE Sum of two ECGs and the Distance between the pacing sites, one could apply the VT RMSE Sum (calculated between the VT and each PM point) to the model to determine how far the VTSO is from each PM point.

5.7.1 – Linear Regression Used for Navigation

During the selection of the ECG analysis metric (Section 5.5), a simple linear regression was used. However, these data sets consisted of large numbers of PM points (see Appendix A). Within the VTSO navigation algorithm, only three PM points are used to triangulate the location of the VTSO, meaning there are only three pairwise points on the RMSE sum – distance plot as shown in Figure 5-7. A pairwise point is defined as a unique PM point pair, i.e. PM1-PM2, PM2-PM3, and PM1-PM3. The RMSE sum and distance are calculated for each pair and plotted. Using a simple linear regression for a set of only three points is often unreliable due to the small size of the data set, resulting in widely varying slopes and intercepts. To fix this problem, the least squares linear regression was constrained to pass through the origin. The code used to calculate the origin-constrained least squares linear regression is available in Appendix B-3.
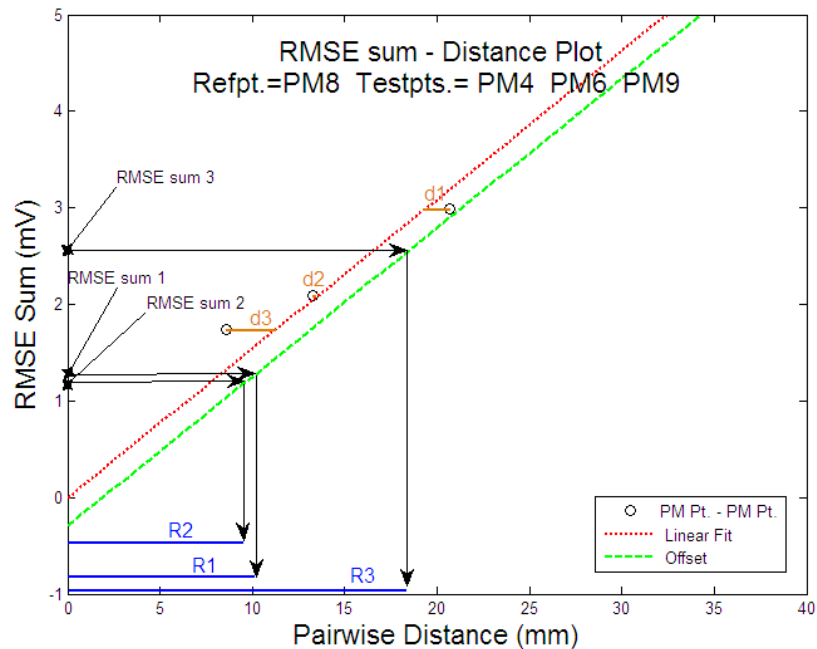
Figure 5-7. Using the shifted linear model to identify the location of the VTSO. The three PM point pairs are represented by the circles. The shifted linear model (green) is determined by the standard deviation of the horizontal distances d1, d2, and d3 to the constrained regression. R1, R2, and R3 represent how far the VTSO is located from each respective PM point. Data is from Patient 9.

Constraining the regression to pass through the origin makes theoretical sense because ECGs recorded for PM points physically located at the same position on the endocardium should produce the same ECG. Therefore, PM points close in distance should have RMSE sum values close to 0. Furthermore, Patient 9's RMSE sum – distance plot for his entire data set had an R value very close to 1.0, making his linear regression an ideal predictive model for determining the location of the VTSO. This ideal data set had an unconstrained linear regression that intersected very close to the origin (Figure 5-4). Therefore, even if we select three PM points for the VTSO navigation algorithm resulting in a small R value, we know the predictive model should

intersect the origin. Therefore, the least squares linear regression for the three points is always constrained.

5.7.2 – Linear Regression Shift

Once the origin-constrained linear regression is made for the RMSE Sum – Distance plot, the RMSE sum is calculated between the VT ECG and each PM point. The approximate distance of the VTSO from each PM Point can be determined by plugging the VT RMSE sum values into the linear model (see Figure 5-7). Let us call these distances R1, R2, and R3. By drawing spheres centered around each of the three PM points with the radii equal to R1, R2, and R3, an intersecting region should appear. This region is the target region that should contain the VTSO. However, assuming there is some variation in the data, the VTSO may appear just outside the target region. To increase the chance of the target region actually containing the VTSO, a buffer region is created which takes into account the variation in data. This buffer region is created by shifting the linear regression to the right, which increases all of the R values hence increasing the size of the spheres and the size of the target region.

The horizontal distance from each RMSE Sum – Distance point to the origin-constrained linear regression is calculated. These distances are labeled as d1, d2, and d3 in Figure 5-7. The standard deviation of these horizontal distances is then calculated, and the line is shifted by ¼ of this value. With this method, plots with a large correlation coefficient result in a small shift, while points with a small correlation coefficient result in a larger shift. The larger shift results in a larger target region since the certainty of where the VTSO is located based on loosely correlated data is smaller compared with the certainty based on a tight correlation.

It is important to note that the size of the shift can be changed to any arbitrary value, as the size of the shift currently used is itself arbitrary. The electrophysiologist may want to increase or decrease the size of the target region for a specific case in order to fine tune the VTSO navigation results. Increasing or decreasing the target region size is accomplished by manually increasing or decreasing the size of the linear shift, respectively.

5.8 – Surface Model Geometry Reconstruction

In Section 5.7.2, it was explained that the target region containing the VTSO is determined by the intersection of three spheres centered around three PM points. The radii magnitudes of the three spheres represent the approximated distance of the VTSO to the PM points. These were calculated from the linear model as shown in Figure 5-7. Although we now have a target region formed by three intersecting spheres, the electrophysiologist still needs a ventricle surface model so that he knows where that target region is located on the ventricle.

5.8.1 – ESI Reconstruction

St. Jude's Medical's ESI system (Section 3.1) automatically builds a surface model of the ventricle based on the continuous (x, y, z) coordinate recording at the catheter tip. As the catheter tip is moved around within the interior of the ventricle, it records a volumetric point cloud that is bounded by the endocardial surface. The ESI system uses a patented algorithm to connect the exterior points of the cloud creating an endocardial surface model. The surface model's vertex coordinates can be extracted at a later time to recreate the surface model for retrospective analysis. However, this model

information is unavailable as a raw data feed for use in our VTSO navigation algorithm. Therefore, it became necessary for us to develop our own surface model reconstruction algorithm.

5.8.2 – Raw Data Surface Model

The raw data obtained during an ablation procedure can only be extracted as the continuous (x, y, z) data from the catheter tip, which provides a volumetric point cloud of data representing the interior volume of the ventricle. For our VTSO navigation program, it was necessary to develop an algorithm that can create a surface model of the heart from this volumetric point cloud of varying point density.

5.8.2.1 – Point Conditioning

The first step requires the user to visually observe the point cloud and remove any extraneous points (this can be done easily with Matlab's brush tool). These points can result when the catheter pops out of the ventricle due to a buildup of tension in the catheter line, or when the catheter tip applies to push pressure against the endocardial wall. An example of some highlighted extraneous points is shown in Figure 5-8 a.
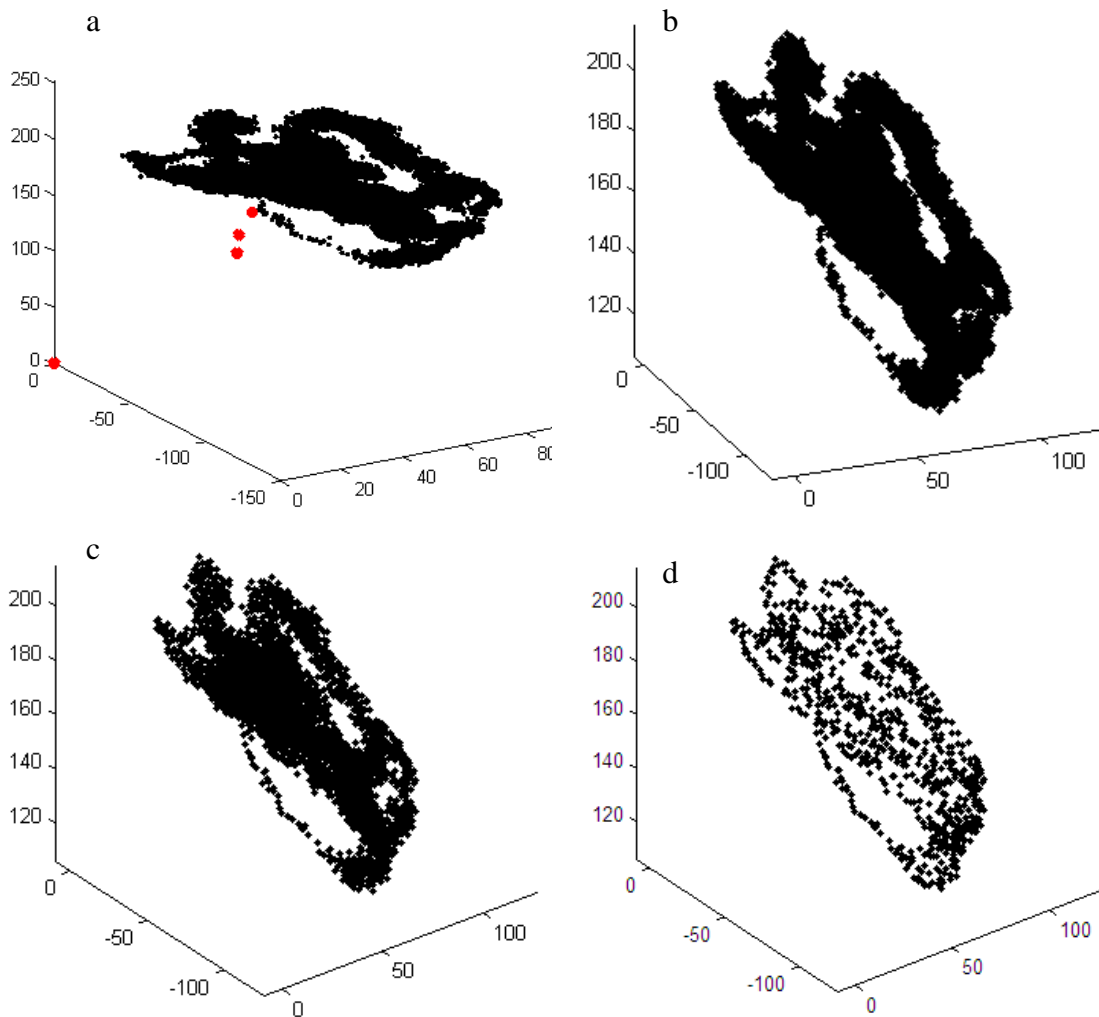
Figure 5-8. Point density reduction process. First, extraneous points like those highlighted in (a) are removed leaving (b). Next, points are removed leaving a minimum spacing of 2 mm resulting in (c). Finally, interior points are removed based on point density resulting in (d).

A typical data set includes a large number of points (> 150,000), and much of the information represented by these points is redundant for our purposes. To make the data set more manageable so that the surface reconstruction algorithm can complete in a reasonable amount of time, the total number of points must be filtered down significantly.

The filtering method chosen removes points to achieve a minimum spacing distance of 2 mm. This distance is arbitrary and can be increased or decreased with the

result being a looser or denser point cloud. With 2 mm spacing, the total points for

Patient 21's data set were filtered from 154244 points to 3323, or ~2% of the original

total points. One issue with this method is that the resulting point cloud's surface may

experience an error of 2 mm. While this error will not significantly influence the overall

effect of the program, it can be reduced using a minimum spacing smaller than 2 mm.

Images of the point cloud before and after this filtering can be seen in Figure 5-8b and c,

respectively. The points in Figure 5-8c may still appear dense due to the size of the point

markers. The filtering code used for 2 mm point spacing is provided in Appendix B-4.

After the density of points was filtered down, the interior points needed to be

removed. Two algorithms were tested. The first was based on center of mass. If the

center of mass of points (CM_i) immediately surrounding a particular point P_i in the point

cloud was close to P_i, it meant that P_i was an interior point and was removed. If CM_i was

beyond a specified distance limit from P_i, it meant P_i was near the surface of the model

and the point was retained. This was repeated for all points P in the point cloud. While

this method worked moderately well, it did not work well in cases involving a single

string of points, such as that seen in the bottom of Figure 5-8c.   The center of mass

method considers these points to be interior and removes them, which is incorrect.

The second method is based strictly on point density. An arbitrary point density

is selected. If a point P_i has a point density D above a certain threshold within a certain

radius R, P_i is removed. D and R are arbitrary and can be changed. While this method

does not remove all interior points, it removes a significant amount and retains all

exterior points including the single string of points in Figure 5-8 c. For a density cutoff

of 9 points per $(4/3)*pi*4^3$ mm^3, the total number of points was reduced from 3323 to

only 824. An image of the point cloud before and after this filtering can be seen in Figures 5-8c and d, respectively. The code for this filtering method is provided in Appendix B-5.

5.8.2.2 – Surface Reconstruction Algorithms

Once the volumetric point cloud has been filtered down to a reasonable density, an algorithm is needed to create the surface model. This algorithm must be able to function with a point cloud that still contains many internal points and with varying point density. A commonly used surface reconstruction algorithm is the Delaunay triangulation. This method creates a triangulation for a set of points so that no points in the set are within the circum-sphere of any triangle. The circum-sphere of a triangle is the sphere that contains all three triangle vertices on its surface. A 2D representation of this definition of Delaunay is shown in Figure 5-9a. Computing the Delaunay triangulation for the point cloud in Figure 5-8d produced the model shown in Figure 5-9b. The model is similar to the convex hull, or envelope, of the point cloud as it prevents convex curves and masks ventricular features. Although constraining a Delaunay triangulation is possible and could improve results, it is not an option due to inconsistent ventricle shapes and relative coordinate axes between patients.   We therefore needed to develop our own unique reconstruction algorithm.
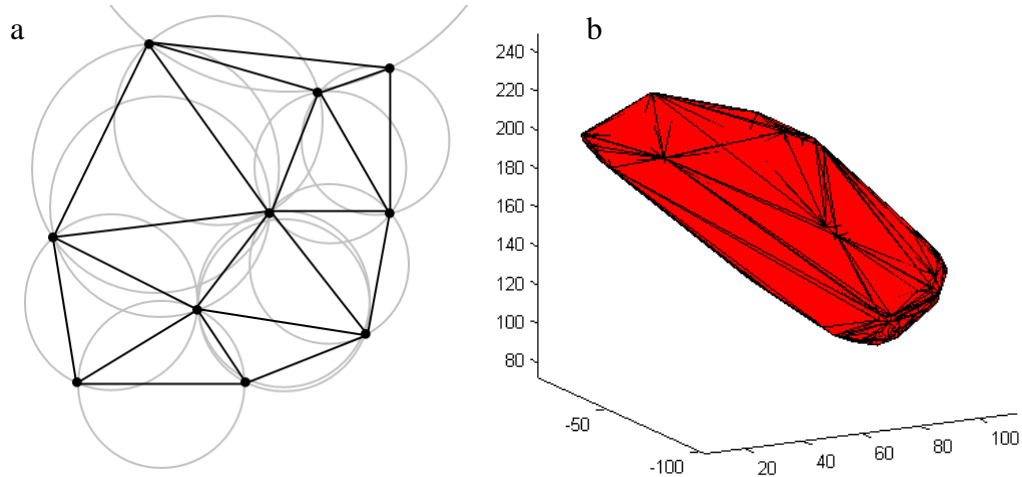
Figure 5-9. 2D Delaunay definition (a) and 3D implementation (b). Figure a uses a few arbitrary points in 2D space to demonstrate how the formed triangles do not lie within any circum-circles (circum-spheres in 3D). Using the Delaunay on Patient 21's coordinate data produced Figure b.

The three methods which produced the best results are as follows. The first involves cycling through all points and creating unique triangles. For each point P_i, unique triangles are created with P_i as one vertex and the two other vertices as points P_1 and P_2 where P_1 and P_2 are within a specified distance D of P_i. Therefore, every point P_i leads to a set of triangles whose sides are no longer than D. When all sets of triangles are plotted together, the geometry of the entire ventricle is observed as seen in Figure 5-10a. D was set at 12 mm for this reconstruction. However, this value is arbitrary and can be changed. Increasing D increases the size of the triangles which reduces any observable holes in the reconstruction, but a large D also reduces the smoothness and accuracy of the edges. While this unique triangles method provided more detailed ventricle features as compared with Figure 5-9b, it required a large number of faces (~235,000 for Figure 5-10a) and did not create a water-tight surface. A water-tight model is defined as an enclosed volume in which every triangle making up its surface is connected on all sides.

49
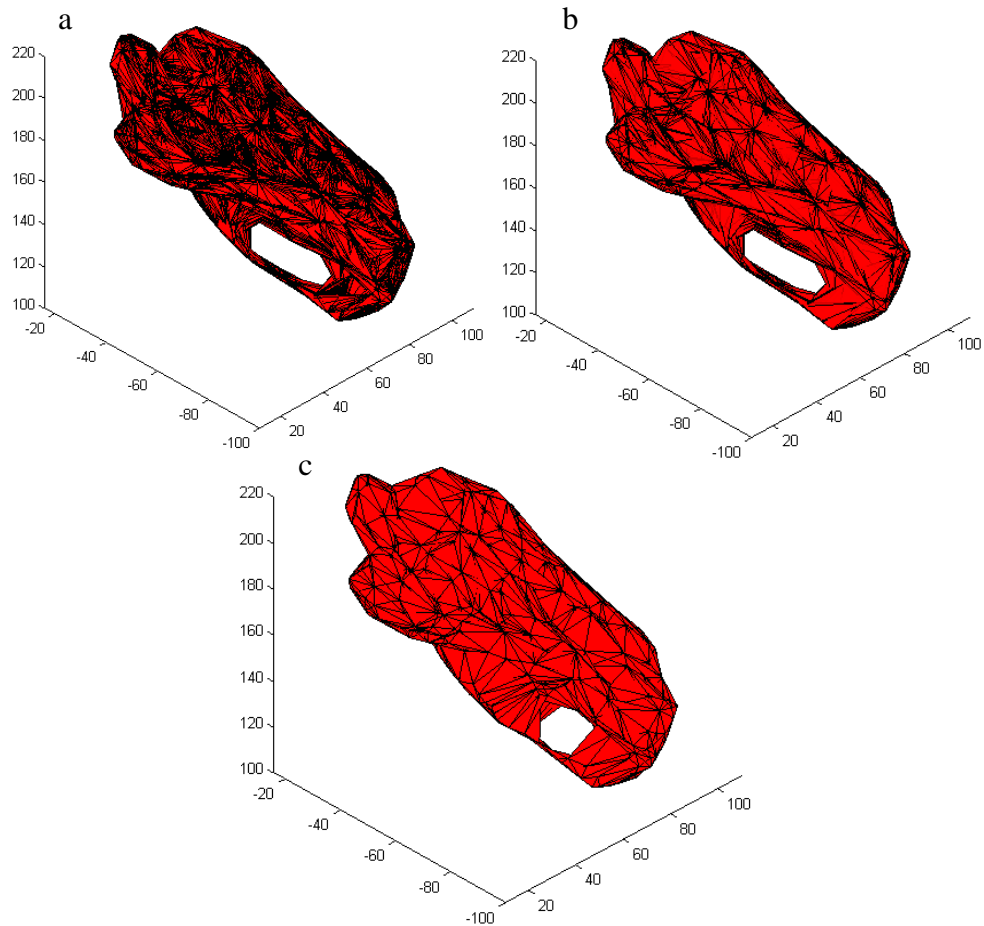
Figure 5-10. Surface reconstruction algorithms. (a) is the result of an algorithm based on unique triangles. (b) is based on combined Delaunay shells. (c) is based on removing large faces of a Delaunay triangulation.

The second method aimed at reducing the number of polygons involved in creating the surface. Like the triangle method, this algorithm cycles through all available points. However, instead of unique triangles, it creates a Delaunay triangulation from the points within a certain distance limit D of each P_i. It then removes the interior surfaces of the Delaunay triangulation, leaving only a shell. Therefore, a small (size based on D) Delaunay shell is created for every point P_i in the point cloud. When all of the shells are plotted together, the geometry of the entire ventricle is observed as seen in Figure 5-10b. Like the unique triangles model, the Delaunay shells model retained ventricle features well compared with the normal Delaunay triangulation shown in Figure 5-9b. It was able

to keep the ventricle features while reducing the number of faces from ~235000 in the triangle method to ~26000 – a reduction of 89%. While this is an excellent improvement, like the unique triangles method it failed to create a water-tight surface.

The final method aimed at creating a water-tight surface and involved modifying a single Delaunay triangulation. The normal Delaunay triangulation does create triangles that connect and outline desired features of the ventricle. However, it also creates large triangles that mask these features. These large triangles are apparent in Figure 5-9b. Therefore, removing triangles with sides beyond a certain length should reveal the smaller triangles making up the actual surface of the ventricle. Computing the normal Delaunay triangulation for the point cloud and removing triangles with sides greater than 16 mm resulted in the model shown in Figure 5-10c. The 16 mm length limit is arbitrary and can be changed. Increasing the length limit reduces surface detail but also reduces the size of potential holes in the model. Like the previous two methods, this modified Delaunay method retained the ventricle features, but it also created a water-tight surface model. Furthermore, the total number of triangles was reduced to ~8000, a 70% reduction from the Delaunay shells method and a 97% reduction from the unique triangles method. The number of triangles may be further reduced since the model currently includes some internal polygons. The code for this final method is displayed in Appendix B-6. This was selected as the final algorithm for surface reconstruction as it created a surface model with acceptable feature detail, required the fewest number of triangles, and formed an enclosed surface.

5.9 – VTSO Surface Model Target Region

With the VTSO target region selected as explained in Section 5.7.2, and the surface model created (Section 5.8), the surface model can be color coded to better highlight the target region and direct the electrophysiologist to the VTSO location within the ventricle. In Section 5.7.2, the target region was described as the intersection of three spheres with each sphere centered on one of the three PM points and having a radius equal to the expected distance from the VTSO to that particular PM point. We now apply these three spheres to the surface model. If a part of the surface model is within all three spheres, it is highlighted red. If part lies within two spheres, it is highlighted yellow. Lying within one sphere is identified by blue, and white indicates not lying within any spheres. The result is a color gradient model in which the target region containing the VTSO is highlighted red, and regions in yellow, blue, and white are less likely to contain the VTSO. An example of this is shown in Figure 5-11. In this figure, the green circles represent the three PM points and the purple circle is a fourth PM point representing the location of the VTSO.
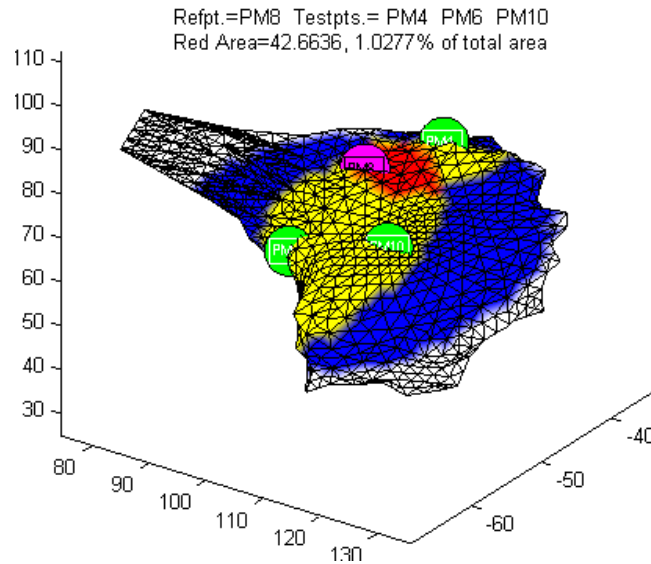
Figure 5-11. Color-coded identification of the VTSO target region. For this particular test, a PM point was used in place of the VT and is marked in purple. The three PM points used for triangulation are marked in green. Data is from Patient 9.

5.10 – Average Ventricular Linear Regression (AVLR)

While some patient data sets provide tight linear correlations (high R values), which in turn result in excellent VTSO triangulation results, other patients produce RMSE Sum – Distance plots showing a large amount of variance in their data. This is attributed to a number of reasons, including nearby scar tissue, PM points at opposite sides of the ventricle, poor digital ECG recording, and human error. In some cases, one of the three PM points used for triangulation may be faulty due to some combination of the above factors. For the VTSO navigation process to proceed at an efficient pace, the program needs to rapidly identify which of the three PM points, if any, are contributing to poor or misleading results. Such identification would allow the electrophysiologist to quickly select a new PM point at a different location to replace the unreliable point, hopefully improving the triangulation results in the process. In order to locate the

53

misleading point, the program needs a reference to compare against. By the end of a pace mapping procedure, enough data points have been collected to create a RMSE sum – distance reference. However, at the beginning of a procedure for a new patient, no unique RMSE Sum – Distance reference exists. To enable interpretation of how reliable initial PM points are, the average ventricular linear regression (AVLR) was created.

The AVLR was created by computing the origin constrained least squares linear regression as well as the 90% prediction intervals for 12 patients, including 14 ventricles. The slopes of the regressions and the offsets of the prediction intervals for each ventricle were averaged to create the AVLR and its 90% prediction interval. An example of an RMSE Sum – Distance plot utilizing the AVLR is shown in Figure 5-12. Instead of simply averaging the slopes and offsets, one would expect some sort of weighting system in calculating this AVLR based on the number of data points available per patient. In most studies, a larger data set indicates more reliable information, so it is weighted more. However, for our studies, all the data sets are from different sources which contain unique sizes and scarring patterns. Therefore, no single data set better represents a normal patient's ventricle. Therefore, weighting was not used.
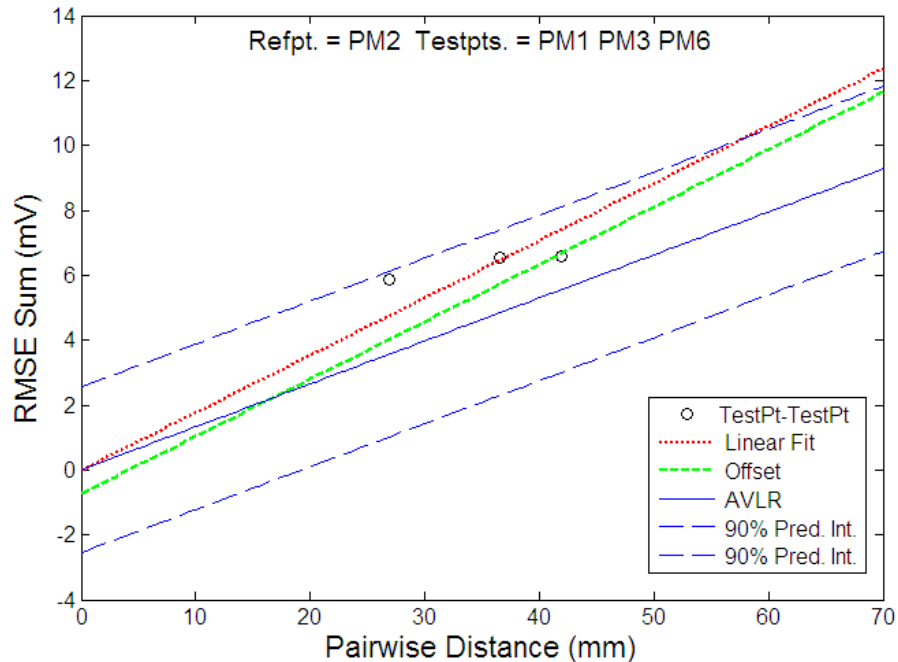
Figure 5-12. AVLR used for the VTSO triangulation algorithm. The solid blue line is the AVLR, the dashed blue lines are the 90% prediction intervals calculated using GraphPad Prism software (GraphPad Software, Inc., La Jolla, CA), the red dotted line is the constrained least squares regression for the 3 PM points, and the green line is the offset of that regression. Data is from Patient 4b.

The circular points in Figure 5-12 are the RMSE Sum – Distance points for the unique pairing of the three PM points, i.e. the RMSE sum and distance were calculated between PM1-PM3, PM3-PM6, and PM1-PM6. If an RMSE Sum – Distance point is located outside of the 90% prediction intervals, a warning is sent to the user. The program uses this point, and the point second furthest from the AVLR to determine which PM point is the contributing factor to the potential error. Even if all the plotted points lie within the 90% boundary, if the red VTSO target region on the surface model is beyond a usable size (the program sets this arbitrary limit as >15% of the total surface area), then the program uses the two plotted points furthest from the AVLR to determine which PM point is the likely cause of the problem. For example, if the two plotted points are from PM1-PM2 and PM2-PM3 comparisons, then PM3 is marked as the likely culprit

for producing poor results. The user is suggested to remove PM3 and use a new point for the next triangulation.

However, it is important to note that these program warnings are merely suggestions. In Figure 5-13a below, since two points were outside the prediction interval, the program suggested replacing a test point with a new point. However, note the tight linear correlation of the data. A high R value usually leads to excellent surface model results. In Figure 5-13b, the surface model contains only a sliver of red target area, correctly predicting the location of the reference point. Therefore, the user should only consider the test point changes suggested by the program if they do not trust or cannot use the surface model results. Additional examples of how the AVLR and surface model results are used to locate the VTSO are provided in Section 5.11.
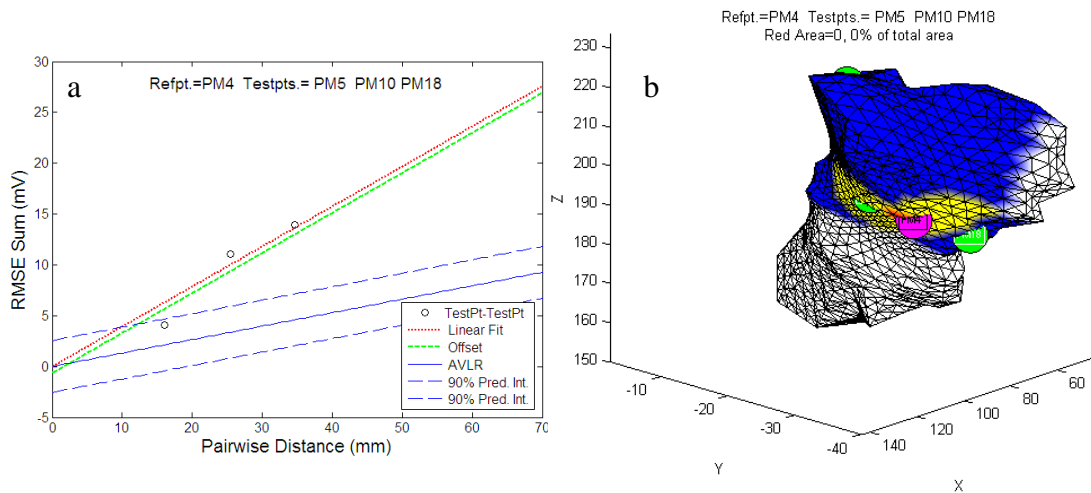

Figure 5-13. AVLR limitations. Although the plotted RMSE Sum − Distance points are outside of the AVLR prediction interval (a), they are still strongly correlated and accurately predict the location of the reference point (b). Test points are green and the reference point, representing the VTSO, is purple. Data is from Patient 15.

5.11 – Retrospective VTSO Navigation Experiments

With the available ECG and geometry data recorded and all aspects of the VTSO navigation algorithm functioning as explained in Sections 5.1 through 5.10, retrospective studies were performed using clinical data. This means the ablation procedure and recording of the data was performed at a prior time to the actual tests. However, these tests were conducted with the mindset of what the doctor had to work with during the ablation procedure. Although these retrospective tests are limited by the available data, such as the number of PM points recorded during that actual ablation procedure, they are the next best thing to real time clinical tests. In many tests, a PM point ECG and location is used in place of the VT ECG template and VTSO location because the VTSO ECG or location information was not recorded. The PM point acting as the VT is referred to as the reference point and is marked in purple on figures. The three PM points used to triangulate the position of the reference point are referred to as test points and are marked in green on figures. The following retrospective studies show how the VTSO triangulation program functions under different circumstances and how the results should be interpreted.

5.11.1 – VTSO Triangulation with Ideal Patient Data Sets

In some studies, the RMSE Sum – Distance data is strongly correlated with an R value greater than 0.9 such as the data compiled from Patient 9 (see Figure 5-4 and Table 5-1). For ideal sets of data like Patient 9's, the VTSO navigation algorithm performs exceptionally well. It identifies a small and accurate target region regardless of where the test points are located. Figure 5-14 shows two tests from an ideal data set using different reference points and tests points. Both tests identify a small target region which contains

57

the reference point. If the reference points had been the actual VTSO, the electrophysiologist would have located the VTSO using the first three PM points he acquired.
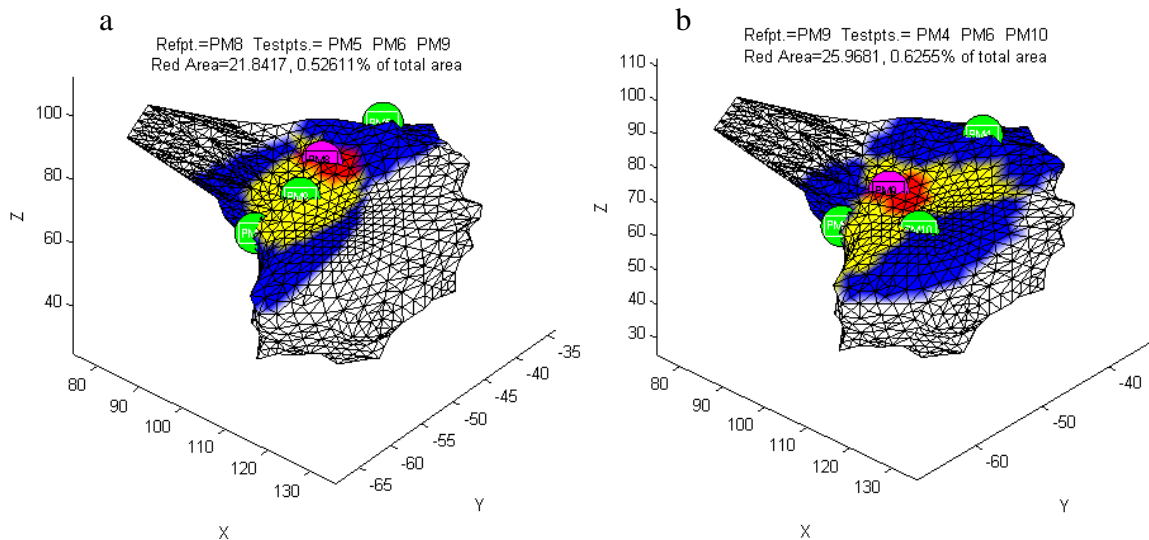
Figure 5-14. Triangulations using an ideal data set (R value close to 1). Test points are marked by green discs, and the reference point is marked by a purple disc. These are two retrospective tests using different reference points and different combinations of test points from Patient 9.

Even if all three test points are positioned away from, not surrounding, the reference point, the target region still provides excellent information on where the reference point is located. As illustrated in Figure 5-15a, if the three test points are not surrounding the reference point, and the target region contains a test point near its center, then the reference point should be located at the border of the target region furthest from the center of mass of test points. Figure 5-15b shows a retrospective test from Patient 9 demonstrating this logic. Even if a patient has loosely correlated data (low R value), this type of logic can still be used to guide test point selection and ultimately highlight a small and accurate VTSO target region. Cases involving loosely correlated data sets are discussed in Section 5.11.2.
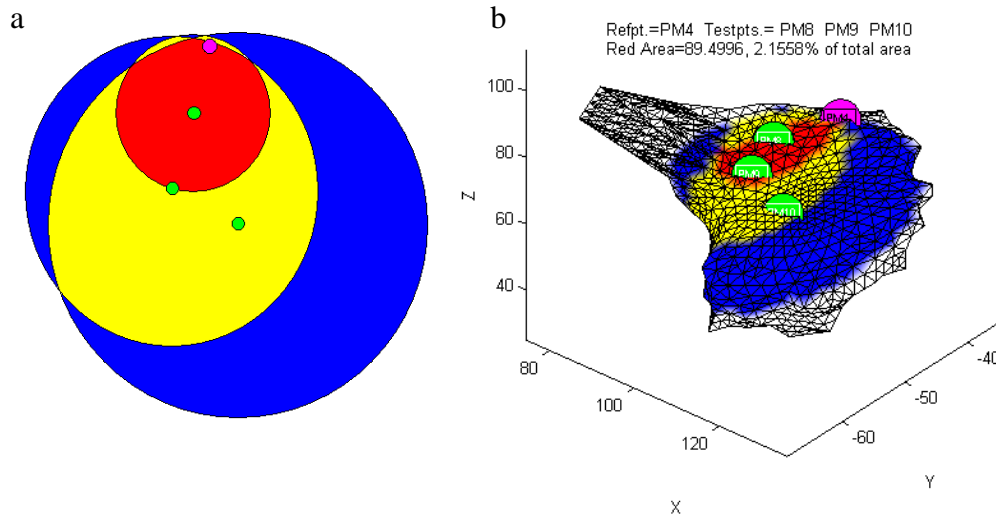
Figure 5-15. Interpretation of target region results. (a) is a 2D illustration of how the reference point should be located at the target region border away from test point center of mass. (b) is a retrospective test using Patient 9's data.

5.11.2 – VTSO Triangulation with Low R-value Data Sets

For high variance data sets like the one seen in Figure 5-5 of Section 5.6, the

VTSO algorithm still produces useful results for the surgeon in locating the VTSO. For

high variance data sets, the algorithm relies on its use of the AVLR and the user's best

judgement when discarding test points and selecting new ones (see Section 5.10). Best

results are achieved when the test PM points are all located on one side of the ventricle

and are surrounding the reference point. In a real case, since the user does not know the

location of the reference point, the selected test points will often be located away from

the reference point and not surrounding it. Therefore, the user must rely heavily on the

AVLR and the logic demonstrated in Figure 5-15.

5.11.2.1 – PM Reference Point and AVLR Reliance

The following example from Patient 15's data set, the user selected three test

points (PM5, PM7, PM21) spanning a large surface of the ventricle. However, the

59

resulting RMSE Sum – Distance plot was loosely correlated and the surface model, shown in Figure 5-16a, highlighted such a large target region (~70% of the total surface area) that it was not particularly useful in identifying the exact location of the VTSO. The algorithm suggested discarding PM17 based on the AVLR. By following these instructions and selecting a new test point (PM4), the R value of the correlation was slightly increased and the target region was slightly reduced to ~50% of the total surface area as shown in Figure 5-16b. Using the AVLR on this output, the program suggested removing test point PM21. By taking this advice and replacing PM21 with PM12, the new linear regression provided a high R value and the resulting target region consisted of only 2% of the total area while accurately containing the reference point as seen in Figure 5-16c. A target region at this level of resolution would be very useful to a physician as a guide to choosing an ablation site.
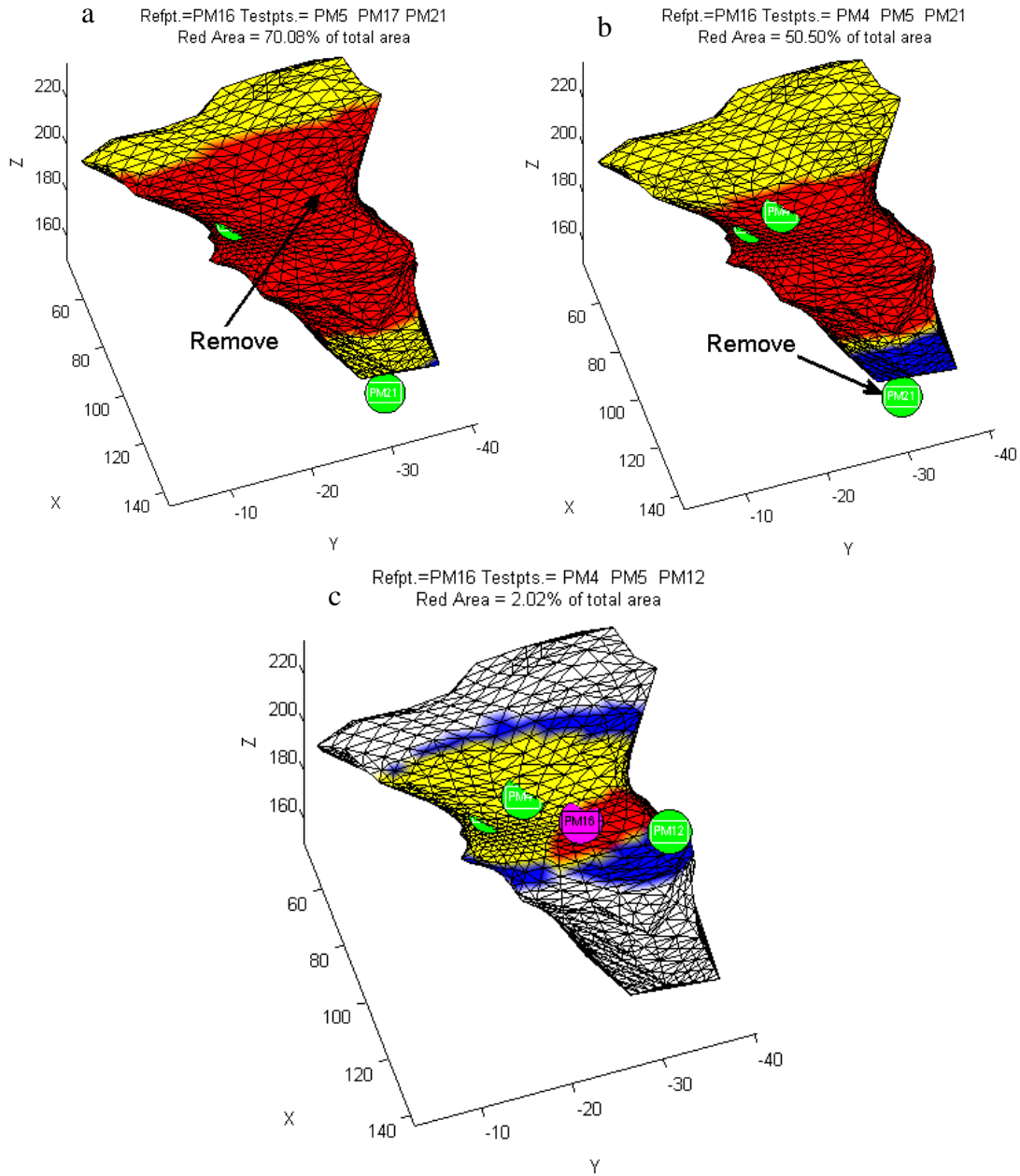
Figure 5-16. Navigation to reference point using AVLR recommendations. Step 1 is shown in (a) with three arbitrarily selected test points. The arrow in (a) points to PM17 which is not visible as it is located beneath the surface of the model at the arrow. Step 2 is shown in (b) with PM17 removed (arrow in (a)) and a new test point (PM4) selected. Step 3 is shown in (c) with PM21 removed (arrow in (b)) and a new test point (PM12) selected. The final target region is shown to accurately contain the reference point marked in purple. This data is from Patient 15.

5.11.2.2 – Clinical VT Reference Point

The navigation described in this section uses the patient's VT as the reference point, which better represents an actual ablation procedure. The VTSO in this case is located at the base of the ventricle, far from most available test points. This meant that the VTSO was not surrounded by most combinations of test points, similar to the situation illustrated in Figure 5-15. However, using AVLR recommendations and the logic described in section the latter half of Section 5.11.1, the user can still navigate to the location of the VTSO in only a few steps.

For this test, the three arbitrarily selected test points (PM3, PM4, PM8) produce the model shown in Figure 5-17a. The large target region has a test point in its central area, and another test point located on the boundary of this region. This positioning is similar to that seen in Figure 5-15 and suggests that the VTSO is on the border of the target region furthest from the center of mass of the three test points. Therefore, the test point at the apex is removed (PM3) and a new test point is selected (PM6). The target region for this new combination of test points is still relatively large as shown in Figure 5-17b. Therefore, the user follows the program's suggestion of throwing out test point PM8 based on the AVLR, and selects a new point (PM9) closer to the border of the target region. The results, shown in Figure 5-17c, have a significantly smaller target region at ~5.7% of the total surface area. Additionally, the fact that a test point is located near the center of the target region suggests that the VT is located near the red boundary opposite from the center of mass of the three test points. If the surgeon were to pace along this boundary, he would quickly locate the VTSO highlighted in purple.
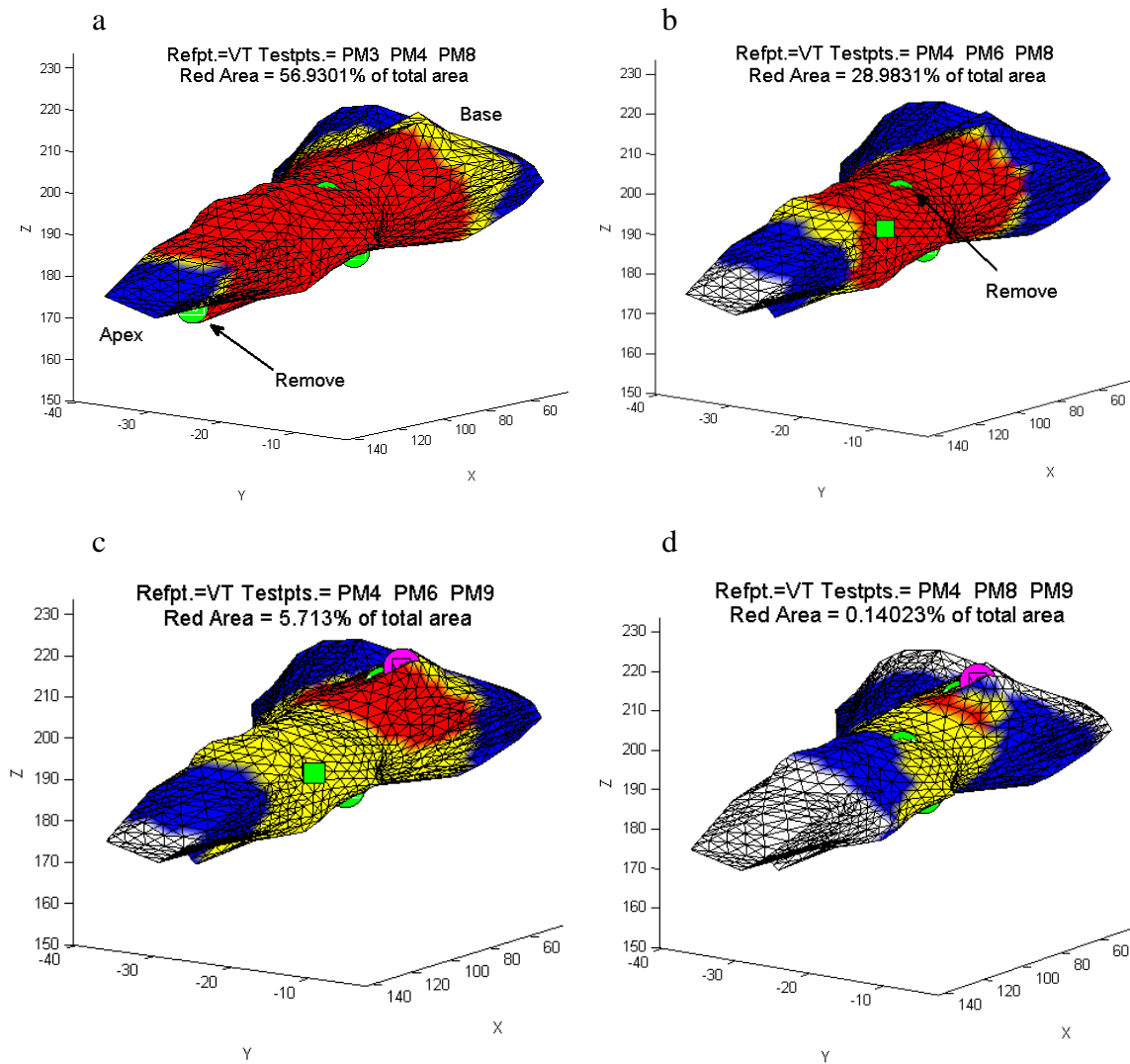
Figure 5-17. Navigation to clinical VTSO. As the first step, three test points were arbitrarily selected as shown by the green markers in (a). Because a test point was located near the middle of the red target area, the VTSO should be located at the border of the target area furthest from the CoM of the test points, meaning PM3 at the apex was the furthest from the VTSO. Therefore, PM3 was removed and a new test point (PM6) was selected as indicated by the square green marker in (b). The navigation algorithm suggests removing PM8 (arrow in (b)) based on the AVLR. A new test point (PM9) is selected in (c) near the VTSO. The electrophysiologist would have little difficulty in locating the VTSO marked in purple using this target area. Alternatively, the user could have removed PM3 in (a) and immediately selected PM9. This would result in the target region of (d). Although the target region is technically inaccurate because it does not contain the VTSO, it is of such a small size and so near to the VTSO that the electrophysiologist would have probably located the VTSO within a few more minutes of pacing.

63

Alternatively, because we guessed that the VTSO was at the basal boundary of the target region in Figure 5-17a, the user could have removed PM3 and immediately selected PM9 as the next test point, resulting in Figure 5-17d. The resulting target region is technically an inaccurate output as the VTSO marked in purple is not located within the target region. However, the size of the target region is so small (~0.14% of the total surface area) and the VTSO is so close that the electrophysiologist would have likely found the VTSO within a few minutes.

Together, these retrospective studies demonstrate the usefulness of the VTSO navigation algorithm in a variety of case types. If the patient produces strongly correlated data, the algorithm will immediately identify an accurate target region of minimal size. If the data is loosely correlated, the AVLR and logic illustrated in Figure 5-15 will guide the user in removing and selecting PM points that ultimately result in a clinically useful target region. Although most retrospective studies were performed with a PM point acting as the VTSO, the studies in 5.11.2.2 showed that the algorithm will function as intended for clinical VT data.

Chapter 6 – Future Work

This thesis remains an early step in the full integration of rapid VTSO localization algorithms into current cardiac ablation procedures. The retrospective tests described in Chapter 5 showed promising results with acquisition of a useful target region utilizing only 3 to 5 PM points total (i.e. up to two steps of removing a PM point and selecting a new one). However, these tests were severely limited in that a PM ECG and location was often used in place of a VT template and VTSO. Furthermore only previously recorded PM points could be used in the algorithm, limiting the choices a user could make when selecting test points. Additional testing to increase the size and completeness of the data sets, including testing of the algorithm during, and not after, the ablation procedures will reveal the true potential of the VTSO navigation algorithm. This will reveal whether the algorithm is ready to be integrated into current Sequential Navigation Systems (SNS) or if modifications in its functionality are in order.

6.1 – Real-time Testing of the Navigation Algorithm

Using raw ECG and geometric data recording software combined with the surface model reconstruction algorithm described in section 5.8.2.2, we should be able to test the VTSO navigation algorithm during an ablation procedure, i.e. in real time. However, there are currently some bugs in the raw data conversion software that interfaces between the medical software and hardware used by the hospital and our computers that run the navigation algorithm. This has resulted in the postponement of these real time tests. However, these bugs are expected to be resolved by early 2012 at which time real time testing can immediately get under way.

6.2 – Additional Testing Sites

Throughout the next year, funding was acquired to facilitate dedicated testing at an additional electrophysiology lab. This is expected to increase our testing rate from 1 patient data set per two months to two or three patient data sets per week. This increased rate of testing should also improve the completeness of the data sets.

Acquiring a complete data set including surface geometry, PM ECG and location information, VT template, and VTSO ECG and location for a single patient is difficult to obtain. It requires excellent communication between the electrophysiologist performing the ablation procedure, the technician operating the SNS who records and labels PM and VTSO ECGs and locations, and the researcher who is extracting the data. It is difficult to maintain this coordination without interrupting the electrophysiologist's normal operating procedures. The patient's health is always a priority over acquiring a full data set. With the increased rate of testing, electrophysiologists and technicians should become more accustomed to including the data acquisition process into current operating protocols. This will undoubtedly result in larger and more complete data sets so that more thorough testing can be performed.

6.3 – Integration into SNS Systems

Based on the results from the retrospective studies described in Section 5.11, St. Jude Medical, Inc. is considering integrating the VTSO navigation algorithm into the research version of their current SNS system – EnSite Velocity. This would provide numerous improvements including user interface familiarity for technicians using the software, access to the detailed ventricle surface model data computed by the SNS system, and instant access to filtered ECG signals. This would also provide a significant

boost to the algorithm's operating speed since the raw data acquired by the medical

hardware no longer needs to be converted into a format readable by our current external

system (Matlab software running on a Microsoft Windows based laptop).

6.4 – Changes to Algorithm Functionality

While the additional testing mentioned in Section 6.2 will hopefully prove that the

VTSO navigation algorithm is an effective tool in quickly localizing the VTSO, it may

instead reveal that fundamental changes to the algorithm's functionality are required. If

this latter outcome occurs, the following changes to the program will be considered. In

some cases, these changes are already being investigated.

6.4.1 – Field Scaling

For the retrospective studies described in Section 5.11, geometric data including

the surface model geometries and PM point locations were automatically modified by the

SNS systems based on patient's physical data such as weight, age, and sex. These

changes were standard to facilitate the use of the SNS. However, the modifications may

have significantly influenced the distance calculations between PM points, influencing

the RMSE sum – distance plots and accuracy of the VTSO navigation algorithm. To

determine to what degree these changes may have influenced the correlations of the

RMSE-sum – distance plots, St. Jude is applying a field scaling algorithm to the original

patient data sets. Once the field scaled data is acquired, new RMSE sum – distance plots

will be made and compared to determine if the R values have improved. If the R values

are improved, the navigation algorithm will provide more accurate results.

6.4.2 – Spherical Shells

Section 5.7.2 described how the target region containing the VTSO is determined by the intersection of three spheres centered around three PM points. The radii of these spheres represent the approximated distance of the VTSO from each PM point based on the shifted linear fit as illustrated by Figure 5-7. The shifted linear fit (shifted right) is used so that the spheres are more inclusive in containing the VTSO. However, as much as the linear fit suggests that the VTSO is not beyond a particular distance (R_o) from a PM point, a left-shifted linear fit would suggest that the VTSO is not within a particular distance (R_i). Figure 5-18a demonstrates how using the shells of thickness t and the particular inner and outer radii would be calculated. A 2D example of the expected improvement in the size of the target area is illustrated in the reduced size of the red region from Figure 5-18b to 5-18c. Although the size of the target region would definitely be reduced, it may also result in a lower overall accuracy of the target region actually containing the VTSO.
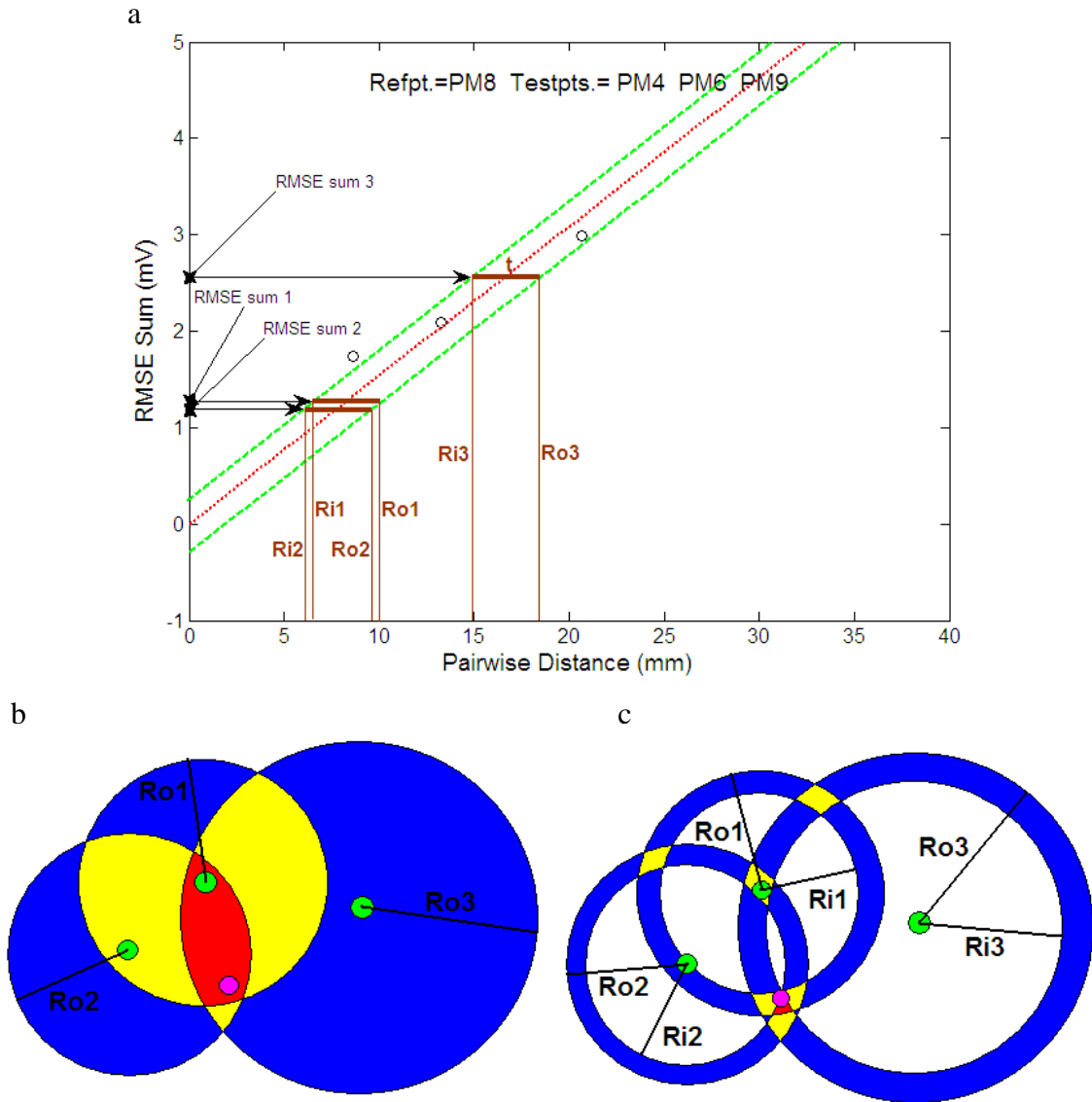
Figure 5-18. Utilizing shells instead of spheres for triangulation. The plot in (a) demonstrates how the shells of thickness t and inner and outer radii Ri and Ro would be determined. The current method uses spheres, as represented by the discs in (b), to triangulate the target region containing the VTSO. By using spherical shells, represented by the rings in (c), the target area could be significantly reduced. PM points are marked in green, and the VTSO is marked in purple.

6.4.3 – ECG Analysis Metrics

Section 5.5 described how four signal analysis metrics were compared and the

RMSE sum was selected as it produced the tightest correlations in the signal analysis –

distance plots. However, some patient data sets still provided correlation coefficients below 0.5 as seen in Table 5-1. Changes in how the signal analysis is performed should be further researched with the hopes of improving these correlation coefficients. In addition to investigating other error metrics besides RMSE, one could try basing the analysis on different subsections of the QRS region instead of the entire QRS segment. Another option is weighting some ECG channels more than others depending on the location of the corresponding PM points. However, this also brings up design considerations such as how the locations of the PM points will be identified, i.e. automatic or user input.

6.4.4 – AVLR Supplement

Instead of relying solely on the AVLR to identify which PM point is throwing off results, the size of each PM point's sphere (distance to VTSO) could also be considered. For example, if a sphere encompasses the entire ventricle, then it fails to add any useful information for the identification of the VTSO, and it's associated PM point should be replaced with a new point.

6.5 – PM Scatter Method

If the PM procedure ends up taking nine or more PM points scattered on all sides of the ventricle, there is an alternative method to selecting and running the VTSO navigation algorithm step by step using three PM points at a time. Calculating the Delaunay triangulation using only the coordinates of the PM points will provide combinations of three PM points that create relatively small triangles along the ventricle surface. In other words, it will not provide combinations of PM points that exist on

opposite sides of the ventricle. As shown in Figure 5-5, this should increase the

correlation coefficients. The VTSO navigation algorithm is then computed using each of

the PM point combinations from the Delaunay, and the resulting target regions are

displayed together on the ventricle surface model. The region of the ventricle with the

highest concentration of target regions may ultimately provide a smaller and more

accurate VTSO target region than using a single combination of three PM points.

These are only a few options that may improve the navigation algorithm's results.

However, they may also needlessly overcomplicate the functionality of the algorithm.

Before significant changes are made to the algorithm, results should be analyzed from the

additional and real-time testing described in Sections 6.1 and 6.2. Based on the

retrospective studies performed thus far, results suggest that the algorithm will perform as

intended without the need for significant changes.

Chapter 7 – Summary of Contributions

7.1 – Navigation to VTSO Using the AVLR

During the course of this project, I have developed an algorithm that uses an average ventricular linear regression (AVLR) and prediction intervals to guide the user in quickly triangulating the ventricular tachycardia source of origin (VTSO). As detailed in Section 5.10, the AVLR was created using 14 ventricle data sets. It provides a reference RMSE Sum – Distance line which the algorithm uses to identify which of the three test points used to triangulate a VTSO target region should be removed and replaced with a new point to improve the triangulation results.

7.2 – Automatic Location of QRS Region

Normal pace mapping (PM) points create a pacing spike, or pacing artifact, immediately before the start of the QRS segment. This helps the user in identifying the beginning of the QRS. However, this pacing artifact is not present in VT ECGs, making identification of the start of the QRS segment difficult. Using the cross correlation sum of the channels between the VT and a PM point, I have created an algorithm that automatically selects the QRS region based on signal similarity as detailed in Section 5.4.

7.3 – Surface Model Reconstruction

In order to test the VTSO navigation algorithm in real time, a surface model of the heart must be created from a variably spaced volumetric point cloud. Most surface reconstruction algorithms are not designed to handle volumetric clouds with significantly uneven spacing. I developed three algorithms that successfully created surface models

while retaining important ventricle features. However, only one created an enclosed

model with relatively few vertex coordinates or polygon faces. As explained in Section

5.8.2.2, this algorithm calculates the Delaunay triangulation for the point cloud and

removes any surfaces with sides greater than a specified length.

7.4 – Retrospective Testing of Clinical Data

I performed retrospective tests of clinical data acquired from ablation procedures I

attended. The navigation algorithm was shown to work effectively for both strongly

correlated and loosely correlated data sets, identifying a small target region containing

the reference point (VTSO or PM point representing the VTSO) using only three to five

test (PM) points.

Chapter 8 – Conclusion

An algorithm for localizing the ventricular tachycardia source of origin (VTSO) has been presented. It has been designed to provide a clinically useful target region with reliability, speed, and ease of use. Electrophysiologists can use the target region, a highlighted area on a ventricular surface model, to rapidly identify the exact location of the VTSO. In order to complete this VTSO localization algorithm, an average ventricular linear regression (AVLR) line was created as a reference for data sets containing low correlation coefficients, a ventricular surface model reconstruction algorithm was created for variably spaced volumetric point clouds, an automatic ECG QRS extraction algorithm was created for VT ECGs, and retrospective testing was performed on 20 ventricle clinical data sets acquired from ablation procedures (Appendix A). Some studies have reported mean ablation procedure times of 383 ± 97 minutes with a mean of 62 pacing points per patient [16]. Based on our retrospective testing of the VTSO localization algorithm presented in Chapter 5, we were able to identify a small and accurate target region using a total of 5 PM points for the data set with the lowest correlation coefficient and a total of only 3 PM for the one with the highest correlation coefficient. With significant amounts of clinical testing expected within the next year, the VTSO localization algorithm will hopefully perform as well as it did during the retrospective tests. It has the potential to significantly reduce total procedural time, reducing costs for the hospital and the patients while improving patient care.

Appendix A – Patient Data Chart

VTSO Patient Data Portfolio

Investigators: Joe Davis, Jerry Wierwille, Keith Herold, Magdi Saba, and Stephen Shorofsky
Clinicians: Magdi Saba and Stephen Shorofsky

Patient #	System	Heart Chamber	Pacing Pts	VT	Other Signals	Geometry	Clipping	Comments
1a	CARTO	RV	16	No	PVC(2)	Yes	No	
1b	CARTO	LV	15	No	----	Yes	No	
2	CARTO	LV	7	Yes (2)	----	Yes	No	
3	CARTO	LV	7	Yes (3)	----	Yes	No	
4a	ESI	RV	8	Yes (1)	----	Yes	Yes	RV PMs 4, 6, 8, & 9 incorrectly labeled
4b	ESI	LV	5		----	Yes	No	
5	CARTO	LV	9	Yes (3)	ECF (1), EMF (1)	Yes		
6	CARTO	LV	8	Yes (2)	----	Yes		
7	CARTO	LV	7	Yes (1)	----	Yes		
8	CARTO	RV	16	No	PVC (1)			Specific pacing points taken for analysis
9	ESI	LV	7		----	Yes	No	
10	CARTO	LV	23	Yes (1)	----	Yes	Yes	
11a	ESI	RV	15	Yes (5)	----	Yes		Most pacing coordinates not recorded (only PM4, 5, & 15)
11b	ESI	LV	4		----	Yes		
12	CARTO	LV	10	Yes (1)	----	Yes		
13	ESI	RV	6	No	PVC (1)	Yes	Yes	
14	CARTO	RV	11	No	----	Yes	Yes	
15a	ESI	RV	13 (no PM10)	Yes(2)	PVC(1)	Yes		No coordinate data for second VT
15b	ESI	LV	21 (no PM13)			Yes		
16	ESI	RV	12	No	----	Yes		Large noise for channels 2 and 3, currently throws off correlation
17	ESI	LV	10	No	----	Yes		Only loc and wav files available - no ECG data
18	ESI	RV	7 and 8	No	PVC(1)	Yes		Only loc and wav files available - no ECG data
19	ESI	LV	18	No	epicardium	Yes		Endo and Epi positions - Only loc/wav files available - no ECG data
20	ESI	LV	20	Yes	----	Yes		ECGs at same locations at different times
21	ESI	LV	~22	Yes (2)	----	Yes		First full raw data set recorded for analysis
Number of Pacing Points:	Mean		14.1429					
	Std.Dev.		5.6886					

Appendix B – Code Segments

B-1

```matlab
for i = 1:length(PMpts)
    crosscorr = [];
    for j = 1:12
        [c, lags] = xcorr(handles.xref1{RefPt}(j,:),
handles.x1{PMpts(i)}(j,:), handles.numdata*2);
        c = c/max(c);
        crosscorr = [crosscorr; c];
    end
    sumcrosscorr = zeros(1,length(crosscorr));
    for k = 1:size(crosscorr,1)
        sumcrosscorr = sumcrosscorr + crosscorr(k,:);
    end
    [C,I] = max(abs(sumcrosscorr));
    index = I - 2*handles.numdata;
    if index > 0
        xref2{i} = handles.xref1{RefPt}(:,index:(index-
1+length(handles.x1{PMpts(i)}))));
    else
        xref2{i} = handles.x1{RefPt};
    end
end
```

B-2

```matlab
%Code segment written by Jerry Wierwille
%Use only the test PM points (PMpts)
for i=1:length(PMpts)
    for k=1:length(PMpts)
        for j=1:12
            %Root Mean Square Error (RMSE)
            sqrdiff_PMpts(j,k,i)=0;
            for n=1:size(handles.x1{RefPt},2)
                sqrdiff_PMpts(j,k,i) =
sqrdiff_PMpts(j,k,i)+(handles.x1{PMpts(k)}(j,n)-
handles.x1{PMpts(i)}(j,n))^2;
            end
            RMSE_PMpts(j,k,i) =
sqrt(sqrdiff_PMpts(j,k,i)/n);
        end
    end
end
%Calculate RMSE sum
for i=1:size(RMSE_PMpts,3)
    for j=1:size(RMSE_PMpts,2)
        RMSE_PMpts_Sum(i,j)=sum(RMSE_PMpts(:,j,i));
    end
end
```

B-3

```
V = [];
x = Distances_PMpts(i,:);
y = RMSE_PMpts_Sum(i,:);
x0 = 0;
y0 = 0;
x = x(:); %reshape the data into a column vector
y = y(:);
%'C' is the Vandermonde matrix for 'x'
n = 1; %Degree of polynomial to fit
V(:,n+1) = ones(length(x),1,class(x));
for j = n:-1:1
    V(:,j) = x.*V(:,j+1);
end
C = V;
%'d' is the vector of target values, 'y'.
d = y;
%There are no inequality constraints in this case, i.e.,
A = [];
b = [];
%Use linear equality constraints to force the curve to hit
the
%required point.
Aeq = x0.^(n:-1:0);
%'beq' is the value the curve should take at that point
beq = y0;
p = lsqlin( C, d, A, b, Aeq, beq );
slope=p(1,1);
intercept=p(2,1);
```

B-4

```
%filter data for 2mm spacing of point cloud
distancelimit = 2; %mm
i = 1;
while i < length(coordinates)
    point1 = coordinates(i,:);
    points = coordinates((i+1):end,:);
    points2 = [(points(:,1)-point1(1)).^2, (points(:,2)-
point1(2)).^2, (points(:,3)-point1(3)).^2];
    distance = sqrt(sum(points2, 2));
    check = distance < distancelimit;
    index = find(check) + i;
    coordinates(index,:) = [];
    i = i + 1;
end
```

B-5

```matlab
%filter out as many interior points as possible based on
point density
j = 1;
distancelimit = 4; %mm
index = [];
index2 = [];
for i = 1:length(coordinates)
    point1 = coordinates(i,:);
    points = coordinates;
    points2 = [(points(:,1)-point1(1)).^2, (points(:,2)-
point1(2)).^2, (points(:,3)-point1(3)).^2];
    distance = sqrt(sum(points2, 2));
    index = distance < distancelimit;
    neighbors = coordinates(index,:);
    numneighbors = size(neighbors,1);
    if numneighbors > 9
        index2(j) = i;
        j = j + 1;
    end
end
coordinates2 = coordinates;
coordinates2(index2,:) = [];
```

B-6

```matlab
%calculate the 3D delaunay triangulation,
%then remove any faces with sides greater than specified
distance (mm)
dt = delaunayn(coordinates2);
distancelimit = 16; %mm
faces = [];
lines = [];
for i = 1:length(dt)
    newfaces = combnk(dt(i,:),3);
    faces = [faces; newfaces];
end
sortedfaces = sort(faces,2);
sortedfaces2 = unique(sortedfaces,'rows');
%p =
patch('Faces',sortedfaces2,'Vertices',coordinates2,'FaceCol
or','r'); axis vis3d;
for i = 1:length(sortedfaces2)
    newlines = combnk(sortedfaces2(i,:),2);
    lines = [lines; newlines];
end
points1 = coordinates2(lines(:,1),:);
points2 = coordinates2(lines(:,2),:);
calculation1 = [(points1(:,1)-points2(:,1)).^2,
(points1(:,2)-points2(:,2)).^2, (points1(:,3)-
points2(:,3)).^2];
distance = sqrt(sum(calculation1, 2));
check = distance > distancelimit;
index = ceil(find(check)./3);
index = unique(index);
filteredfaces = sortedfaces2;
filteredfaces(index,:) = [];
p =
patch('Faces',filteredfaces,'Vertices',coordinates2,'FaceCo
lor','r');
axis vis3d;
```

References

[1] Roger, V. et al. American Heart Association/American Stroke Association Heart Disease & Stroke Statistics 2011 Update. *Circulation.* 2011, 123:e18-e209

[2] Srivathsan K., Lester S.J., Appleton C.P., Scott L., and Munger T.M. Ventricular tachycardia in the absence of structural heart disease. *Indian pacing and electrophysiology journal.* 2005, 5:106.

[3] Chan PS, Vijan S, Morady F, Oral H. Cost-effectiveness of radiofrequency catheter ablation for atrial fibrillation. *J Am Coll Cardiol.* 2006, 47:2513-2520.

[4] Segal OR, Chow AW, Wong T, Trevisi N, Lowe MD, Davies DW, Della Bella P, Packer DL, Peters NS. A novel algorithm for determining endocardial VT exit site from 12 lead surface ECG characteristics in human, infarct-related ventricular tachycardia. *J Cardiovasc Electrophysiol.* 2007. 18:161-168.

[5] Ito S, Tada H, Naito S, et al. Development and validation of an ECG algorithm for identifying the optimal ablation site for idiopathic ventricular outflow tract tachycardia. *J Cardiovasc Electrophysiol.* 2003. 14:1280-1286.

[6] Sanroman-Junquera M, Mora-Jimenez I, Almendral J, Everss E, Caamaño-Fernandez A, Atienza F, Castilla L, JL Rojo-Alvarez JL. Automatic location of ventricular arrhythmia using implantable defibrillator stored electrograms. Computing in Cardiology 2010;37:749−752.

[7] Zhang X, Ramachandra I, Liu Z, Muneer B, Pogwizd SM, He B. Noninvasive three-dimensional electrocardiographic imaging of ventricular activation sequence. Am J Physiol Heart Circ Physiol. 2005;289:H2724–2732.

[8] Guyton A, Hall J. Textbook of Medical Physiology, 11 Edition. W B Saunders Co. 2006.

[9] Robbins J, Dorn GW. Listening for hoof beats in heart beats. *Nature Medicine.* 2000. 6:968 – 970.

[10] Berger M, Sra J, Cooley R, Blanck Z, Deshpande S, Dhala A, Akhtar M. Ventricular Tachycardia. In: Saksena S and Camm AJ. Electrophysiological Disorders of the Heart. Philadelphia: Elsevier, 2005.

[11] Stevenson, William G., Callans, David, d'Avila, Andrea, Kottkamp, Hans, Sosa, Eduardo, Yao, Yan. Wiley-Blackwell. Mapping Methods for Ventricular Tachycardia Ablation 0.1002/9781444317077.ch6. John Wiley & Sons, Ltd.

[12] Pruszkowska-Skrzep P, Kalarus Z, Sredniawa B, et al. Effectiveness of radiofrequency catheter ablation of right ventricular outflow tract tachycardia using the carto system. *Kardiol Pol.* 2005. 62:138–144.

[13] Josephson M, Callans D. Using the twelve-lead electrocardiogram to localize the site of origin of ventricular tachycardia. *J Heart Rhythm.* 2005. 2(4): 443-6.

[14] Szeplaki G., Tahin T., Szilagyi S.Z., OSZTHEIMER I., Bettenbuch T., Srej M., Merkely B., and Geller L.. Ablation of premature ventricular complexes originating from the left ventricular outflow tract using a novel automated pace-mapping software. *Interventional Medicine & Applied Science*. 2010. 2(4): 181–183

[15] Da Costa A. Catheter ablation procedures: role of nation-wide registries. *Europace.* 2009. 11 (2): 133-134.doi: 10.1093/europace/eun354

[16] Yoshida K, Liu T-Y, Scott C, et al. The value of defibrillator electrograms for recognition of clinical ventricular tachycardias and for pace mapping of post-infarction ventricular tachycardia. *J Am Coll Cardiol*. 2010. 56:969-979.